

Strut-Braced Dry Wing Concept for Hydrogen-Powered Aircraft

M. Méheut¹, D. Losada Costoso¹, F. Moens¹, O. Atinault¹, C. Julien², L. Vertonghen², L. Coelho³, V. Priasso⁴, A. Lannoo⁴, S. Defoort⁵, E. NGuyen Van⁵, C. David⁵, D. Glenis⁵, J. Sodja⁶, S. de Boer⁶, J. Schwingel⁷ & D. Eisenhut⁷

DAAA, ONERA, Institut Polytechnique de Paris, 92190, Meudon, France
 DMAS, ONERA, Université Paris-Saclay, 92320, Châtillon, France
 DAAA, ONERA, Institut Polytechnique de Paris, 92320, Châtillon, France
 DMAS, ONERA, 59000, Lille, France
 DTIS, ONERA, Université de Toulouse, 31000, Toulouse, France
 Delft University of Technology, Delft, The Netherlands
 University of Stuttgart, Institute of Aircraft Design, Stuttgart, Germany

Abstract

This paper aims at presenting the design of a LH₂-powered Strut-Braced Dry Wing configuration (SBDW) done within the Clean Aviation UP Wing project for a Small-Medium Range mission (239 PAX, 2500 Nm). In this framework, ONERA, Technical University of Delft and University of Stuttgart are setting up a common multidisciplinary design process to explore the design space offered by such a configuration where the wing no longer bears the function of carrying the fuel as the cryogenic LH₂-tanks are located at the rear of the fuselage. This paper describes first the multidisciplinary and multi-fidelity design process with a detailed description of all disciplinary modules and their integration in the Fast OAD ONERA overall aircraft design (OAD) process. The second part focuses on the analysis of the results with a deep dive into the performance of the optimal concept.

Keywords: LH₂-powered aircraft, Strut-braced wing, dry-wing, MDO

1. Introduction

After several decades of refinement and optimization, the conventional "tube & wings" aircraft concept with kerosene fuel seems to have reached its peak performance and efficiency levels. However, increasingly stringent environmental regulations require going even further in terms of fuel efficiency and reduction in carbon emissions, and it is unlikely that this conventional concept will manage to meet all these requirements. As a result, innovative aircraft concepts have been increasingly studied, that rely on a combination of lightweight structures and novel energy sources. Among those, LH₂-powered aircraft, and Very High Aspect-Ratio (VHAR) wings have been identified as some of the more promising concepts. To raise the challenges of such concepts, ONERA, TU Delft and University of Stuttgart investigate the potential of a LH₂ strut-braced dry-wing (SBDW) concept for a Small-Medium-Range like mission (2500 Nm, 239 PAX, Cruise Mach number: 0.78) to minimize the energy consumption in flight while reducing to zero the CO₂ emissions in the frame of the Clean Aviation UP Wing project.

The combination of both LH₂-powered aircraft and very high-aspect ratio wing features first the need to re-evaluate the nature and positions of fuel storage, so that the wing itself no longer bears the function of carrying the fuel as for LH₂-powered aircraft, the liquid hydrogen has to be stored inside the fuselage, in dedicated cryogenic storage systems, for efficiency and safety reasons. Because of the absence of fuel in the wing, the dry wing option is one of the most promising to drastically change the design paradigm and strongly reduce the energy consumption of future aircraft configurations. With this dry-wing concept, radical new wing structural design layouts are possible. The main change compared to wet wings is twofold. First of all, the fuel tank volume constraint is removed. This opens the avenue for a thinner wing and a completely different wing internal structure. Second of all, the inertia relief is no longer present for the assessment of static loads, and due to the significantly different wing mass distribution, the dynamic loads are also expected to be different.

Furthermore to benefit from the aerodynamic potential of very high aspect ratio wings (AR > 20) without a tremendous wing weight increase, the addition of a strut appears as one of the most promising solutions to obtain the best aero-structural compromise (strong induced drag reduction with a very limit weight penalty). In addition, all these new challenges in the design of a dry wing as compared to a wet wing most likely will also lead to the need for an actively controlled wing for load alleviation and flutter.

The first part of this paper describes the multidisciplinary and multi-fidelity methodology applied for the design of the SBDW concept as well as the design variables defined to explore the design space. The second one details all disciplinary modules and their role in the overall process. The third part presents a detailed analysis of the results obtained so far. The last part focuses on the performance of the selected configuration.

2. Overall methodology

2.1 Context

In the frame of the UP Wing project, a step-by-step approach was defined across different disciplinary streams to progressively learn about the potential performance of the SBDW concept. Two engine options are considered in this study, either a Ultra-High-by-Pass-Ratio turbofan (UHBR) and an Unducted Single Fan open-fan engine (USF). The overall approach for the design of the SBDW concept is described in Figure 1.

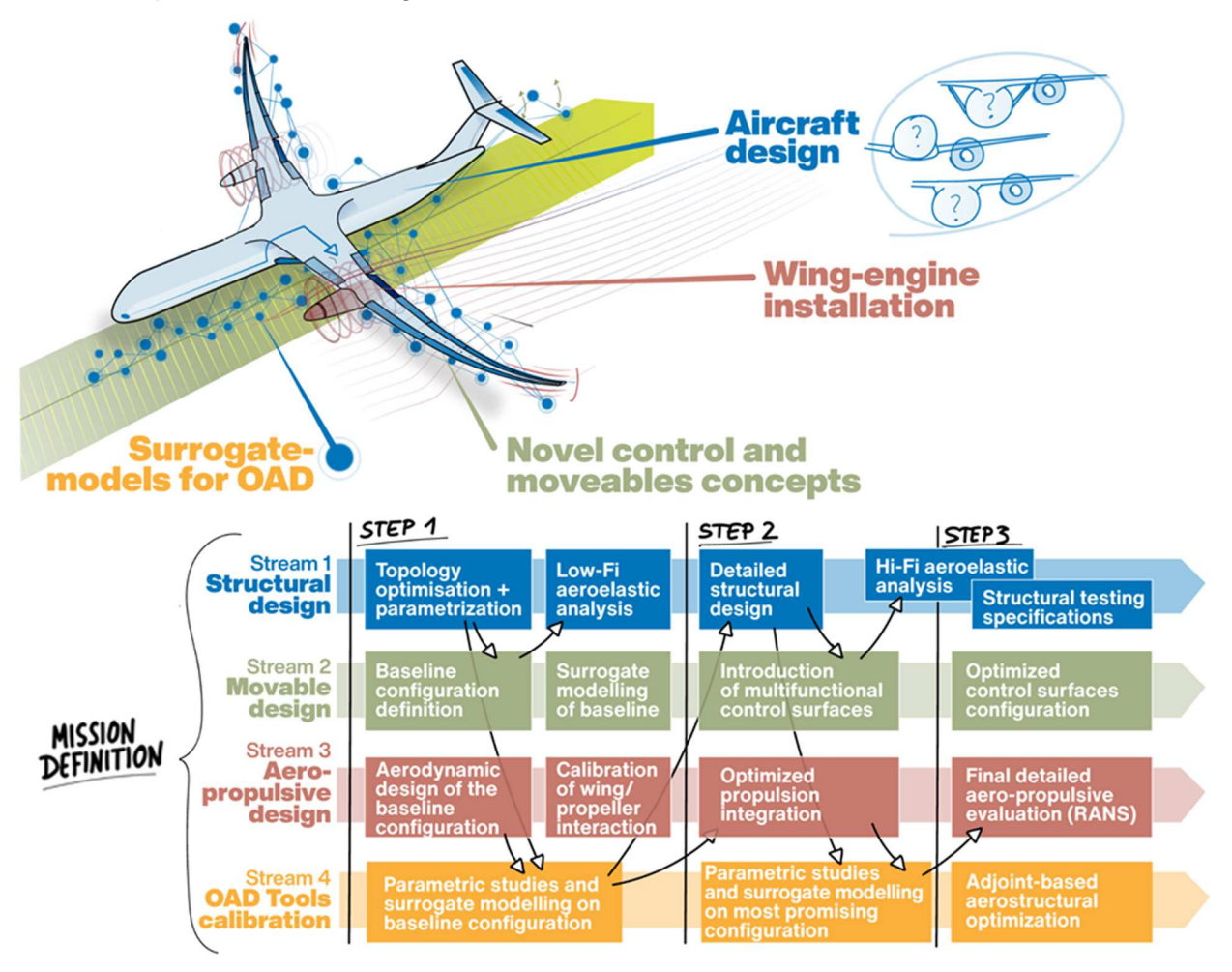


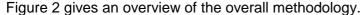
Figure 1 - Step-by-step approach for the design of the SBDW concept in the frame of the UPWING project.

The methodological approach of the SBDW concept development consists in the definition of 3 disciplinary streams which are responsible respectively for the structural sizing, the definition of control surfaces (to ensure handling qualities including load alleviation systems) and the aerodynamic design. The three steps aim at progressively increasing the maturity of the concept as well as the fidelity of tools used for the sizing and analysis of the optimized configuration. **This paper focuses only on STEP1.**

A fourth stream is dedicated to the creation of surrogate models (thereafter RSM) that feed the Overall Aircraft Design process who is responsible for the sizing of the complete aircraft as well as the evaluation of the performance of this configuration.

2.2 Multidisciplinary and multi-fidelity approach

The Overall Aircraft Design process used to design the SBDW configuration is based on the FAST-OAD software developed by ONERA in collaboration with ISAE-Supaero [1][2]. FAST-OAD is an open source software aiming at performing aircraft sizing upon Top Level Aircraft Requirements and user defined parameters, by coupling the relevant disciplines of conceptual aircraft design (aerodynamics, structure, stability and control, propulsion, trajectory and performance). The software and its enhancements towards strut-braced wing and H2 design will be described in §3.1.



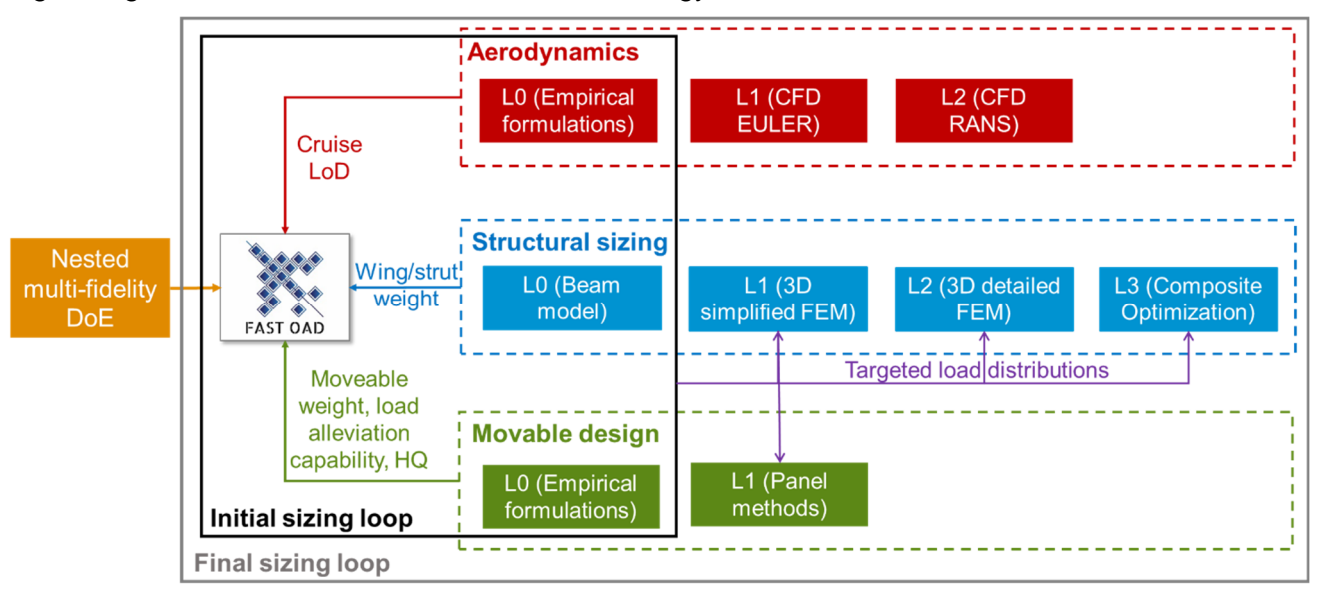


Figure 2 - Multidisciplinary and multi-fidelity design methodology.

The **first step** of this approach is the definition of a large nested multi-fidelity Design of Experiments (DoE) based on key design variables to fully exploit the SBDW design space (see for example multi-fidelity approach described in [4]). For this, 11 variables were defined. They correspond to key characteristics of the wing (Aspect Ratio, root relative thickness and kink location) and of the strut (span, local chords, relative thicknesses and length of the vertical part), and are listed in Table 1. One additional variable represents the height of the fuselage as previous internal studies have demonstrated potential energy consumption benefits with a large fuselage for LH₂ powered configuration (with LH₂ tank located at the rear of the fuselage). Another one represents the mass of the engine in order to include in the design space different engine options such as a classical high-pass ratio engine or an advanced unducted single fan engine which has a significantly higher weight compared to classical engine. The last design variable (LAF) aims to mimic the impact of load alleviation systems on the sizing load cases for the structural wing and strut sizing (from a conventional load distribution up to a very aggressive law). The geometrical parameters are described in Figure 3. The description of the LAF variable is proposed in Figure 4.

	Design variables	Minimal value	Maximal value	
WING	Aspect Ratio - AR	18	28	
	Root relative Thickness - t/cwingroot	10%	13%	
	Relative kink location (% half wing span) - Y_k	20%	90%	
STRUT	Wing / Strut junction (% half wing span) - $Y_{strut} = L_{strut} / \frac{b}{2}$	35%	70%	

Strut-Braced Dry Wing Concept for Hydrogen-Powered Aircraft

	Relative chord at wing junction (% of local wing chord) - $RC_{strut_tip} = \frac{C_{strut_tip}}{c_{wing_strut}}$	40%	80%
	Span of the horizontal part (% half wing span) - $Y_1 = L_1 / \frac{b}{2}$	10%	30%
	Chord ratio at the end of the horizontal part (ratio between the root and wing junction chords) - $CR_{Y1} = \frac{c_{Y1} - c_{strut_tip}}{c_{strut_root} - c_{strut_tip}}$	0	1
	Length of the vertical part (m) - H _{strut}	0.15	1.0
FUSELAGE	Height of the fuselage (m) - H _{fus}	4.2	5.5
ENGINE	Masse of the engine (kg)	5200	8700
LOAD	Load alleviation factor (ratio between the cruise and a targeted spanwise load distributions - LAF	0	0.6

Table 1 - Design variables for the SBDW concept.

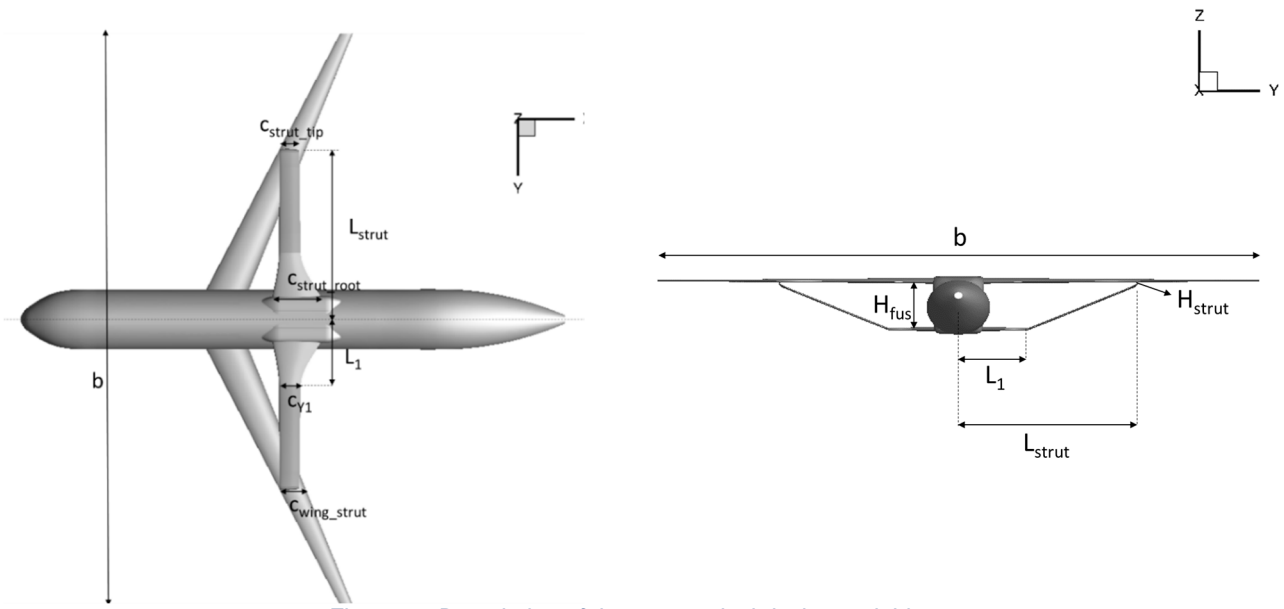


Figure 3 - Description of the geometrical design variables.

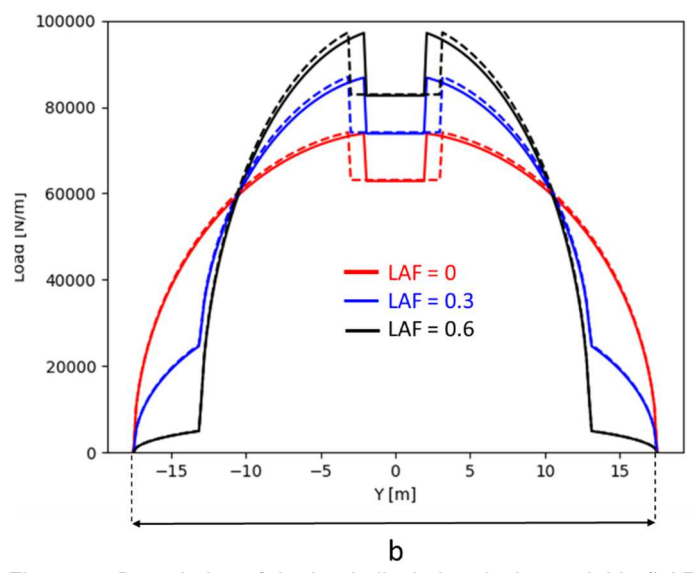


Figure 4 - Description of the load alleviation design variable (LAF).

Strut-Braced Dry Wing Concept for Hydrogen-Powered Aircraft

This DoE is composed of the 1280 configurations with 8 nested levels of fidelity. Between each level, the number of configurations is divided by a factor of 2, meaning that the LEVEL1 includes all the points of the DoE, the LEVEL2 half of these points (640) up to the LEVEL8 which is composed of 10 configurations. This large number of levels was defined in order to let the possibility to adapt the number of configurations evaluated by each high-fidelity disciplinary modules according to the restitution time.

The **second step** of the approach aims at using the low-fidelity models which are natively included in Fast OAD to size all configurations included in the DoE. The results of this initial sizing process is provided as inputs for all high-fidelity modules (described in §3) and considers a description of the geometry of the 1280 configurations as well as the spanwise characteristics of the beam model used in this initial loop for the structural sizing (inertia and stiffness).

During the **third step**, all high-fidelity disciplinary modules evaluate the performance of each configuration corresponding to the level of fidelity selected for the module.

For the aerodynamic stream, the objective is to evaluate the Lift-over-Drag ratio (LoD) in transonic cruise condition (Mach Number of 0.78) and at the MMO (Maximum Operating Mach Number - 0.82) for the different lift coefficients (C_L). This stream is composed of three levels:

- L0 module based on empirical formulations: it is natively included in Fast-OAD, so all configurations are evaluated with this module.
- L1 module based on CFD Euler simulations: 80 configurations (LEVEL5) are evaluated with this module as it is quite time consuming (a few days for the 80 configurations).
- L2 module based on CFD RANS simulations: 20 configurations (LEVEL7) are evaluated with this approach as manual operations are needed to trigger potential flow separations with specified Karmans at the junction between the strut and the wing (particularly critical in transonic conditions)

For the structural sizing stream, the objective is to size the wing and strut structures to provide to the OAD process relevant wing and strut weights. This stream is composed of four modules:

- L0 module based on beam modelling: it is natively included in Fast-OAD, so all configurations are evaluated with this module.
- L1 module based on a simplified Finite Element Model (FEM): 1280 configurations (LEVEL1) are evaluated with this module as it is very efficient in terms of running time.
- L2 module based on an aeroelastic sizing of the structural elements in a detailed Finite Element Model (FEM): 20 configurations (LEVEL7) are evaluated with this module as the complexity of the model requires potential manual operations to provide relevant weights.
- L3 module based on tailoring the geometric and material properties of the structural elements in a detailed Finite Element Model (FEM): only 10 configurations (LEVEL8) are evaluated with this module as this approach relies on size and composite optimisation which can prove relatively time consuming.

The third stream (moveable sizing) aims at evaluating the weight of the moveable based on their sizing, verifying the handling qualities of the configuration and the feasibility of the target load distributions using the different control surfaces for load alleviation (maximum LAF value achievable for each configuration).

- L0 module based on empirical formulation: it is natively included in Fast-OAD, so all configurations are evaluated with this module.
- L1 module based on the doublet lattice method (DLM): 10 configurations (LEVEL8) are evaluated with the model as it uses inputs coming from the L2 structural sizing module and the complexity of the model may require manual operations.

During the **fourth step**, all disciplinary modules provide outputs that are used to create the multifidelity Reduced Surrogate Models (RSMs) based on the SMT toolbox [3]. In the **fifth step**, these RSMs are used by Fast-OAD to resize (final sizing loop in Figure 1) all 1280 configurations of the DoE and evaluate their performance in terms of energy consumption. The **last step** aims at selecting the most relevant configuration in the DoE or defining a new one based on various optimization strategies.

All disciplinary modules used in this methodology are described in the next section. In the current

paper, the results of first three steps are detailed, as all high-fidelity results are not available yet.

3. Overall Aircraft Design process and disciplinary modules

3.1 Fast OAD: a modular Overall Design Process

This section mostly refers to the design capabilities description introduced in [5];

Integrated OAD activities have been running at ONERA for a long time, but the existing tool suites were either based on commercial integration software, or not modular enough to perform MDO studies. Therefore in the frame of Clean Sky 2 and additional internal studies, and taking benefit of on-going internal studies on MDO, a large effort was undertaken to define a new, modular, evolutive tool to conduct the configuration studies, first at L0 level.

A first, simplified version of the tool called FAST (Fixed-wing Aircraft Sizing Tool) was initiated and is shared with ISAE-Supaero. An enhanced version calibrated and improved with ONERA internal knowledge has then been developed under the name of MYSTIC (Figure 5).

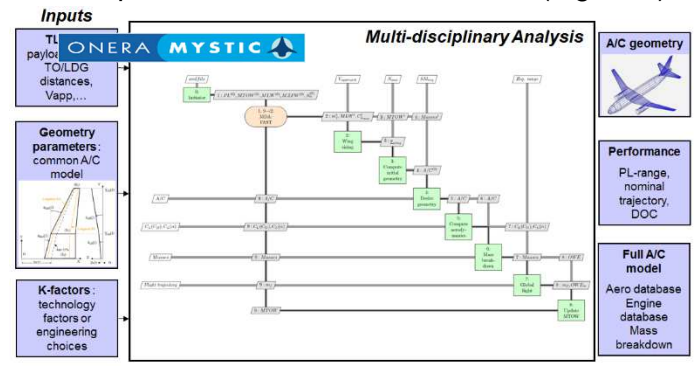


Figure 5 - Inputs and outputs of the MYSTIC tool.

This tool incorporates physical modules for the classical disciplines of Overall Aircraft Design: Propulsion, Aerodynamics, Mass breakdown and balance, Handling qualities, Trajectory and Performance. 3 sizing loops are implemented, allowing to design an aircraft upon its TLARs (Top Level Aircraft Requirements) with iterations on the disciplinary modules:

- Loop 1: design of HTP and VTP surfaces upon trimmability and stability criterions (handling qualities) at take-off and in cruise, iterating on the CoG (Centre of Gravity) position,
- Loop 2: iteration on the wing position to ensure a desired static margin, after calculation of aerodynamic centre,
- Loop 3: iteration on the maximum take-off weight (updated after OWE (Operational Weight Empty) and mission fuel calculation) and wing size (to ensure required approach speed and accommodate the mission fuel).

Finally, along the project, the MYSTIC code was progressively improved and modularized, leading to the FAST-OAD software jointly developed with ISAE-Supaero. This code provides an open source basis that can address conventional configurations, and a collection of proprietary modules dedicated to specific disciplines or configurations. It has been progressively enhanced to address a wide range of configurations with sufficient fidelity level (Figure 6).

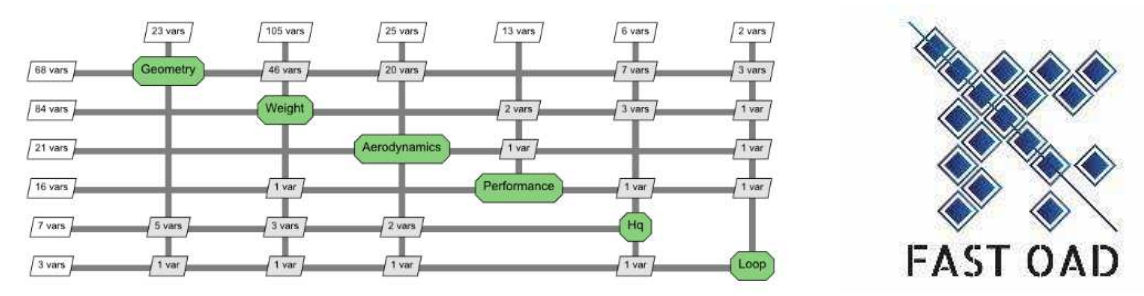


Figure 6 - FAST-OAD multidisciplinary analysis process [2]. Further developments of the software were internally conducted at ONERA within the GRAVITHY project [5][6] to be able to model a hydrogen-powered aircraft (in particular the design of the LH₂ tanks in the fuselage), and within the

U-HARWARD Clean Sky 2 project to implement L0 models for the design of a strut-braced wing configuration [1]. This enhanced H₂-SBW version is used in the frame of this study with gravimetric index of 0.5 for the design of the LH₂ tanks for all configurations evaluated in this paper

3.2 Aerodynamics

The first stream is dedicated to the detailed aerodynamic and aero-propulsive design and performance assessment of the SBDW concept with a special care to the potential synergies between the Dry-Wing concept and the engine integration (UHBR or USF engine). During STEP1 (see Figure 1) special attention is paid to the junction between the wing and the strut, where the constraints imposed by transonic cruise conditions become particularly stringent.

3.2.1 L0: analytical formulations

The level 0 aerodynamic module used in the OAD process is based on analytical formulations derived from either theory or data analysis of past and present aircraft. It has been developed for a fast evaluation of the aerodynamic performance of standard Tube and Wing, Flying Wing, or Blended Wing Body configurations, considering subsonic flight conditions [8] for its use within an OAD process. It starts from the geometry of the reference wing and assumes an optimum elliptical span loading. Then the different elements (fuselage, winglets, nacelles, etc.) are considered as extra components that affect the overall wing performance. Geometrical details, as the airfoil shape, camber or twist, are not taken into account at this stage of the aerodynamic evaluation and are considered in a next step of the design process using more advanced methods. The slope of the $C_L(\alpha)$ curve is estimated by the Polhamus formulation [9] with the effects of fuselage taken into account [10]. The drag formulation retained is derived from [11]:

$$C_{D Total} = C_{D Induced} + C_{D Viscous} + C_{D Wave} + C_{D Parasitic}$$

The lift induced drag coefficient is based on the standard formulation with a combination of both Anderson [12] and Hörner [13] methods for the estimation of the Oswald factor. Fuselage or winglets are considered according to Nita formulations [12] with an adaptation to take the winglet cant angle into account. The contribution of the tail surfaces to the lift induced drag is not considered.

The viscous drag of the different aircraft elements are calculated using the methodology described in [10] and [11]. It considers a turbulent flat plate friction drag (obtained by the compressible Schlichting relation) combined with a form factor for the given element (using [10] for the fuselage, [14] for the wing, the tail surfaces and the winglets and [15] for the nacelles). Fuselages with an elliptical cross section and external tanks can also be considered. For the wing, an additional profile drag due to lift is considered, based on [15] and for nacelles or external tanks, an interference coefficient is considered to account for the surface proximity [10].

Due to the transonic flight conditions of the aircraft mission the drag increase due to compressibility effects is considered using the Korn equation [11]. Finally, an additional parasitic drag due to protuberances, antenna, probes, paint, etc. is assessed, considering a ratio of 2.5% over the friction and pressure drag.

3.2.2 L1: CFD EULER

The L1 aerodynamic module is based on a 3D aerodynamic framework [1] for evaluating the performance of each configuration. As shown in Figure 7, this 3D aerodynamic framework consists of 4 steps.

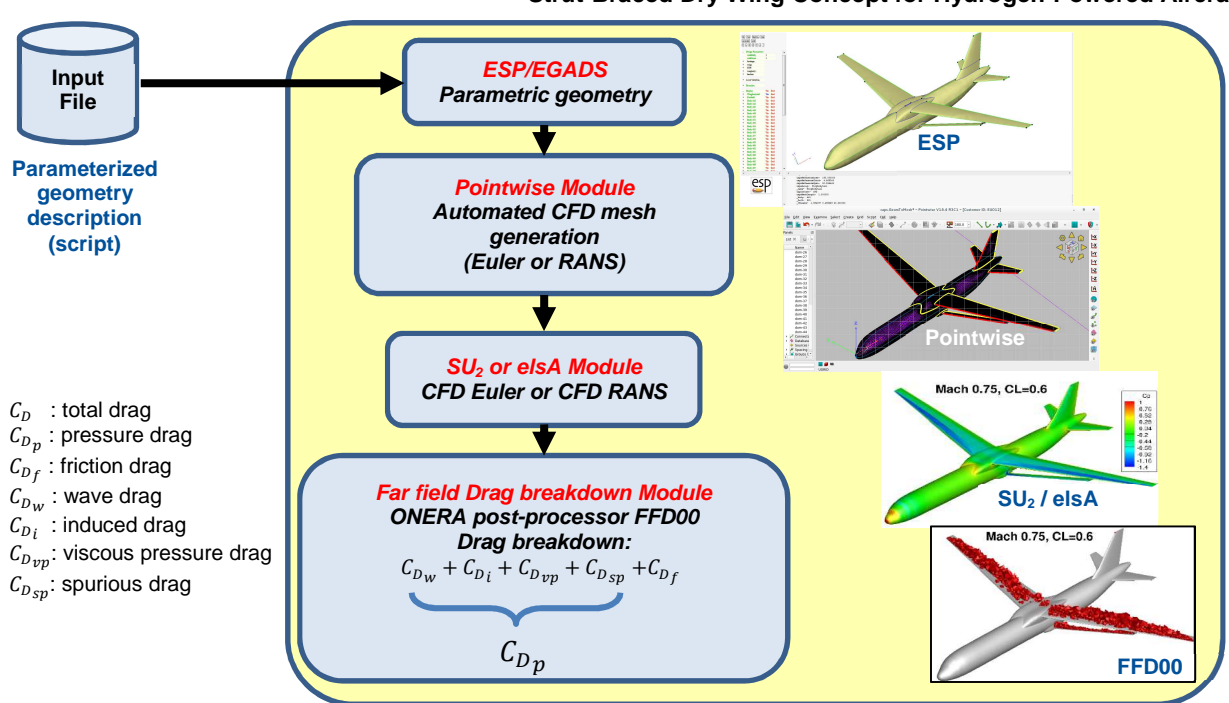


Figure 7 - 3D aerodynamic framework used for multi-fidelity DOE levels 1 and 2.

Firstly, a fully parametric geometry model has been generated using the Engineering Sketch Pad (ESP) tool developed by MIT [16]. Secondly, this geometry is automatically meshed with the Pointwise commercial software. The mesh generated is an unstructured mesh. Following this meshing step, the CFD EULER computation is performed using the SU2 or the in-house elsA (ONERA-SAFRAN property) solver [17]. Finally, the ONERA far-field drag (FFD) post-processing tool provides drag decomposition [18]. For EULER calculations at L1 fidelity level, the $C_{\rm D\it{Viscous}}$ term from the equation presented in section 3.2.1 is added to the global drag.

3.2.3 L2: CFD RANS

The L2 aerodynamic module is based on the same 3D aerodynamic framework as the L1 module presented in §3.2.2, but here, the CFD computations performed are based on RANS formulation. It is therefore unnecessary to estimate the viscous effects by the use of low fidelity analytical formulations. The ONERA far-field drag post-processing tool FFD00 analyses the CFD-RANS results and evaluates wave, induced and viscous drag components.

3.3 Structural sizing

This second stream focuses on the structural design of the Dry Wing concept based on composite optimization together with an automatic structural sizing process. In particular, this stream aims at obtaining the appropriate structural stiffness distribution, along with aeroelastic effects, of the very high aspect-ratio wing as well as the strut, in order to withstand a set of relevant aerodynamic loads, with a detailed assessment of the different junctions (strut-wing, wing-fuselage, strut-fuselage). In addition, a first aeroelastic evaluation of the optimized concept is proposed using low-fidelity aeroelastic analyses for flutter and coupled CFD/CSM static simulations.

The lower fidelity structural levels (L0 to L2), used in the initial and final sizing loops, consider only isotropic materials, while the higher fidelity optimization procedures make use of the anisotropic properties of the composite layers. For the sake of consistency across all fidelity levels, a so called 'black aluminium' fictitious material has been used for the structural sizing of an equivalent isotropic wing and the strut. The properties of this material are derived from a quasi-isotropic (QI) lay-up $[0^{\circ}/\pm 45^{\circ}/90^{\circ}]$. The base ply properties are $E_{11}=149$ GPa, $E_{22}=10$ GPa, $E_{12}=5.2$ GPa, $E_{12}=0.302$, and a density of 1590 kg/m³. Material allowables are defined by a maximum ply strain of 3500 $\mu\epsilon$ in compression and 10000 $\mu\epsilon$ in tension. The resulting equivalent properties of the QI material are: E=57.24 GPa, E=1.84 GPa, E

3.3.1 L0: Beam model

As exposed above, the initial version of FAST-OAD relies on semi-empirical formulas for weight estimates and aerodynamics, in order to account for strut-braced wing configurations, new loads, weight estimates and aerodynamic models have been integrated within FAST-OAD framework.

First, a load evaluation module has been set up to compute both limit and ultimate load factor (n_z) considering a safety factor imposed by the user, typically 1.5. So far, only one load case is implemented that consist in a pull-up manoeuvre at MTOW. Then, specific sub-models are developed to compute the external and corresponding internal loads resulting from aerodynamic, fuel distribution, engines, structural weight itself and introduced by the strut. Only the aerodynamic loads computation is mandatory, the choice for the consideration of other contributions is let to the user.

Once the loads have been properly assessed for all aircraft components, the wing primary structure can be sized. The wings and struts primary structure weights are computed using physical analytical models based on beam theory [19], while the weight of the other parts (fuselage, tails, systems, engines, ...) are assessed through the semi-empirical formula already implemented in FAST-OAD. For the new physics-based models developed here, the wing structure is simplified to an equivalent spar plus skin model with the spar flanges supporting bending moment, the web supporting the shear and the skin supporting the torsion.

This methodology has been extended to the struts considering they only support traction. The models developed here are only valid for isotropic materials. For those materials we consider the tensile yield stress, the compressive yield stress, the maximum shear stress, the density ρ and a minimum technological thickness for metallic sheets, whose typical value is around 2 mm.

Finally, the total wing weight is computed adding the contribution of skin, flanges and web and considering also ribs and secondary parts through empirical formulations. The ribs are supposed to be evenly spaced spanwise with a constant thickness fixed by the used. The secondary structure is computed with the following formula:

$$W_{wing,sec} = 0.3285 \cdot k_{wing} \cdot MTOW^{0.35} \cdot S_{cantilever} \cdot k_{mvo}$$

with k_{wing} and k_{mvo} that are respectively a correction coefficient depending on engine layout (its value is 1 for 4 engine aircraft, 1.05 for two engines and 1.1 for rear engines) and a "cultural" coefficient to take into account structural additional weights. $S_{cantilever}$ is the cantilevered surface of the wing (outside fuselage).

3.3.2 L1: Simplified Finite Element Model (FEM)

The simplified finite element model uses physical equations to obtain accurate properties of the structure prior to calculation, providing a fast estimation (less than ten seconds) of its mass, centre of gravity and inertia (see [20]). The inputs of the model are the planform of the wing, the load cases, the MTOW and the maximum landing weight (MLW). From this data, it minimizes the mass of the wing while ensuring that there is no break (in case of composite material), plasticity (in the case of aluminium for example) or buckling of the main components of the wing (ribs, spars, skin and stringers).

To reduce the mass, many properties of the structure can be modified and tested, such as the space between the ribs and the thickness of the main components. For the optimization loop, the properties of the components are initialized using standard values found on existing aircraft. The lift forces determined in the aerodynamics section have an elliptical distribution and are applied to the wing and a linear finite element simulation is then performed using two-dimensional elements (with 6 degrees of freedom on each node). Using the strains and stresses on each element, the Von Mises criteria (or Tsai-Hill in the case of composites) is then calculated for each component. The thickness is then optimized to avoid the plasticity (or failure for a composite) and the buckling. As the properties of the components are changed, the stiffness of the structure is also changed. Another finite element simulation is then performed with the new properties and so on until the mass of the wing converges and stabilizes. As the calculation is linear, this iteration process is quite fast and still accurate as the properties of the structure are defined using physical equations. The model's output provides the wing's deformation (Figure 8), mass balance and optimized internal structure.

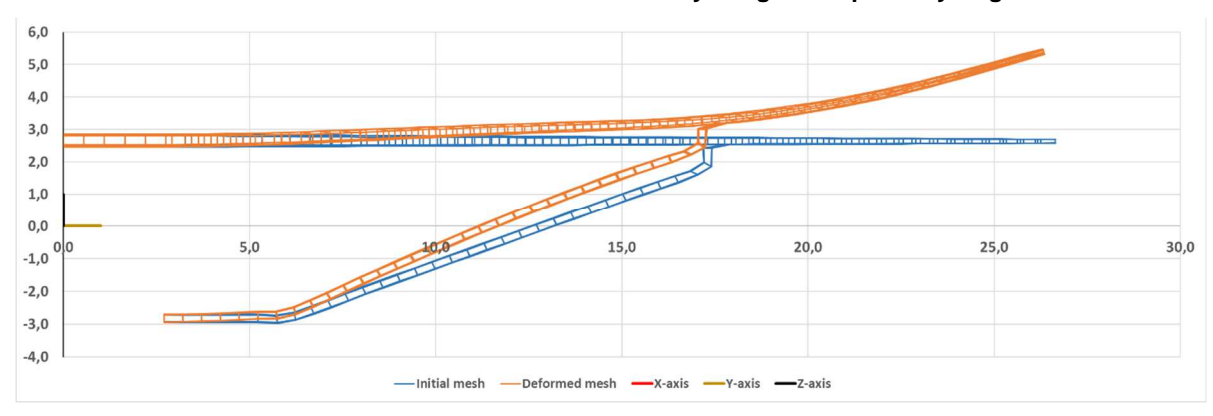
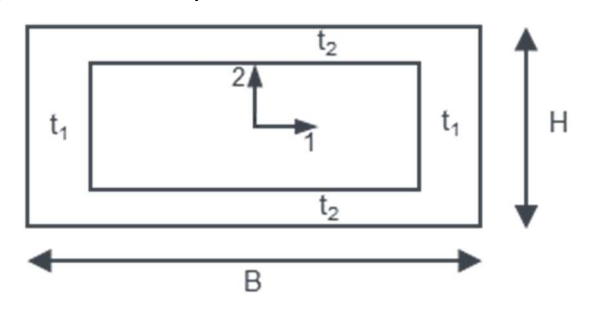


Figure 8 - Initial and deformed mesh for the simplified finite element model.

In parallel of this simplified Finite Element Model developed by ONERA, a dedicated module was created for the strut by University of Stuttgart in order to obtain more robust and complementary results. The strut design is simplified to the strut box modelled with beam elements to allow a fast variation of the design parameters in the low-fidelity step. To achieve this, a framework using ANSA/META and the ABAQUS solver is set up to run through all DoE design points in an automated way. Since the global parameters of the strut are defined in the DoE (such as chords and kink positions), the framework optimize the local thickness distribution of each element for a box cross shape.

In addition to the elliptical lift distribution on the wing, a surrogate load for a strut lift is implemented as a constant C_l load. Based on a cruise $C_L = 0.6$ of the overall aircraft and a lift increment of the flat plate $\frac{dC_L}{d\alpha} = \frac{0.175}{deg}$ at $M_{\infty} = 0.78$, this results in a change in Angle of Attack (AoA) of 5.14° for 2.5g and -6.86° for -1g. Assuming an equal change in AoA for the strut and following the design decision of zero lift on the strut in the design point the lift coefficients on the strut are $C_L = 0.9$ in 2.5g and $C_L = -1.2$ in -1g. With the simplification of the constant C_l , this results in the local lift coefficient C_l being equal to the global C_L .

The wall thickness of the box webs and flanges are computed analytically by solving a simple system of two equations.



$$0 = W_1 - M_1/\sigma_{yield}$$

$$0 = W_2 - M_2/\sigma_{yield}$$
using

$$W_1 = \frac{1}{6H} (BH^3 - (H - 2t_2)^3 \cdot (B - 2t_1))$$

$$W_2 = \frac{1}{6B} (HB^3 - (H - 2t_2) \cdot (B - 2t_1)^3)$$

Figure 9 - Principal box shape for the optimization.

As a constraint, the Euler buckling formulas for a pinned configuration are used to compute the minimum required second moment of area. For this, the axial compression load in each of the three strut sections is applied. Now, two constraints for material failure due to bending and stability exist to minimize the mass of the strut.

3.3.3 L2: LowFi aeroelastic sizing

The L2 structural model is based on the aeroelastic sizing of the SBDW wingbox. The first step consists in generating the aeroelastic model. The inputs for this process are the planform of the wing (i.e. sweep, span and chord distribution) and the mass distribution. The generation of the internal structure of the wing is based on the slicing of a simplified CAD model of the wing. This procedure is interfaced with the Python API of FreeCAD. The structural objects that constitute the wingbox are obtained as slices of the modelled external geometry. The wing box is constituted of ribs, spars, skins and stringers modelled as plate elements, except for the stringers that are modelled as beams. The strut remains modelled by means of a beam element with a hollow

rectangular cross-section. The outer dimensions of the rectangle are fixed, in such a way to maximize the moment of inertia along the chord of the airfoil, serving as fairing. This inertia term is beneficial both because it increases the buckling load and but it also decreases the bending strains. The strut taper is included by successive beam elements with the cross-sectional properties of the smallest cross-section of the element. Then, a doublet-lattice modelling (DLM) of the aerodynamics is built within MSC NASTRAN to complete the aeroelastic model (see Figure 7).

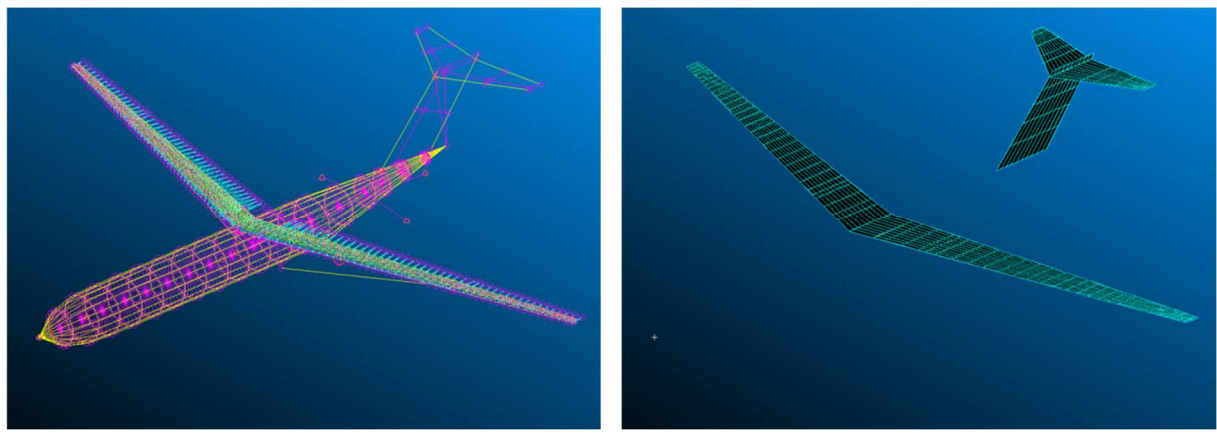


Figure 10 - Aeroelastic model of wings with beam struts. Structure (left) and aerodynamics (right).

The second step performs the aeroelastic sizing within the MSC NASTRAN suite, by using their optimization toolbox. The objective is to minimize the overall structural weight while considering a set of constraints to satisfy. For each bay of the wing, i.e. the space between two consecutive ribs, the design variables are the thicknesses of the upper and lower skins, the thicknesses of the spars, the ratio between the web/flange thickness τ of the stringers (see Figure 8). The "T"-shaped stringer parameters λ is fixed to 5. Finally, the strut design variables are the inner thickness at wing and fuselage junction. Then a linear section variation is done between wing and fuselage junctions. The 'black aluminium' material detailed in §3.3.3 is used.

During the optimization loop, the wing and strut are designed under two types of constraints. Each element is sized to sustain the aeroelastic loads from a stress point of view, using the Von Mises criterion and to ensure the buckling stability of the overall structure. Each constraint has to be satisfied in a set of given load cases at M=0.78: 1g and -1g that come from static aeroelastic computations within NASTRAN and the +2.5g condition with load alleviation (see §2.2).

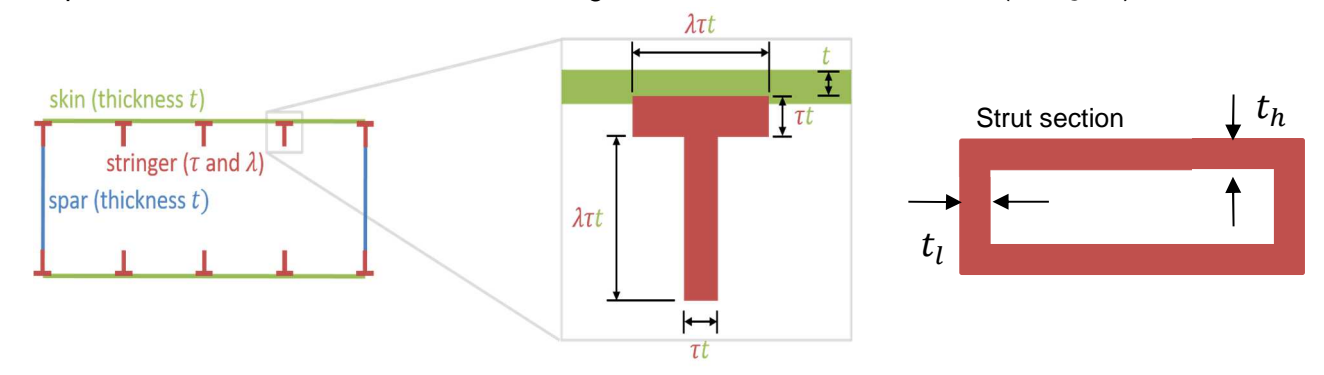


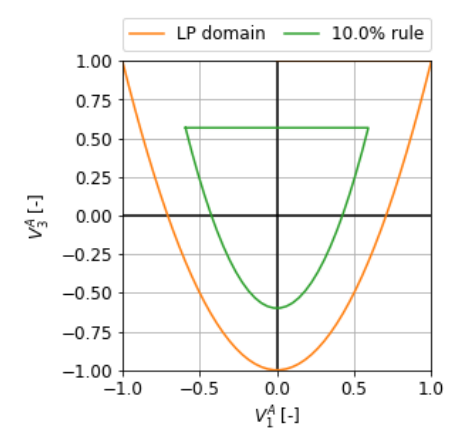
Figure 11 - Wingbox and strut parametrization.

3.3.4 L3: Composite Optimization

This module builds upon the L2 FEM module to perform the local optimization of the composite stacking sequences across structural elements of the wing (upper and lower skin, spars and ribs). At any given point, the composite lay-up is seen as an equivalent homogenized anisotropic material, described by its thickness and a set of material parameters (the Lamination Parameters, thereafter LP [21]). In the general case, there are twelve LP, but under the hypothesis of balanced, symmetric laminates, using a sufficient amount of 0/90/45/-45 layers, then only two parameters (V_1^A and V_3^A) are needed to describe the in-plane properties of the laminate, and two other for the out-of-plane properties (V_1^D and V_3^D). Alongside the thickness, this gives a total of five variables for the composite optimization problem. These five variables are defined locally at each element of the structure.

Practically, they are used to define the PSHELL properties of each stiffened bay, similarly to §3.3.3, and as shown in Figure 6. Furthermore, L3 makes a distinction between the variables for the front and rear spar, and assigns a separate thickness value to each rib.

A minimal ply share of 10% for each of the $[0^{\circ}/\pm 45^{\circ}/90^{\circ}]$ orientations is enforced, by constraining the feasible domain of the V_1^A and V_3^A [22], as shown in Figure 5. Moreover, compatibility conditions between the in-plane and out-of-plane LP are taken into account [23]. These conditions reduce the LP design domain further, but they are necessary to ensure that any given set of LP does correspond to a feasible lay-up.



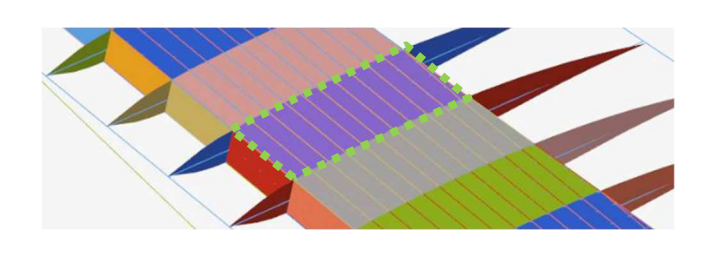


Figure 12 - In-plane LP design domain, and corresponding 10% [$0^{\circ}/\pm 45^{\circ}/90^{\circ}$] ply share domain.

Figure 13 - PSHELL and PBAR property distribution, each color is linked to a set of variables (thickness and LP).

Stiffeners, however, are parametrized differently. A constant and fixed lay-up is used for all the stiffeners, consisting of 70/20/10 shares of $[0^{\circ}/\pm45^{\circ}/90^{\circ}]$ plies respectively. An equivalent shear modulus G and longitudinal Young's modulus E are obtained from the normalized in-plane A matrix of this stacking sequence. They are then assigned to the stiffeners' PBEAM elements with the T cross-section (see §3.3.3). Considering only the in-plane behaviour of these elements is appropriate as the stiffeners are situated far away from the neutral axis of the wingbox and are predominantly loaded axially.

A general buckling constraint is applied by means of a generalized linear eigenvalue problem for the complete structure. Additionally, the strain allowables of the base ply are considered, with the tensile-compressive dissymmetry described in §3.3. Nonetheless, these allowables are defined at the ply scale, while the plies are not described explicitly when using the homogenized LP. Therefore, rather than in the fibre direction, the maximum strain constraint in applied to the minor and major principal strains of the shell elements. In case of the stiffener, only the axial strain is used for the constraint. Finally, the minimal and maximal strains for the strut are obtained by a combination of bending and axial strains at the outer corners of the rectangular cross-section.

As with the L2 structural optimization, the load cases considered during the optimization are the +2.5g condition with load alleviation (see §2.2), and the additional +1g and -1g condition coming from an aeroelastic analysis, at MTOW, all 3 cases with an additional safety factor. These analyses are obtained with a static aeroelastic computation coupling a FEM and a DLM within the MSC NASTRAN suite. The +1g load case serves to design the wingtips in case of large load alleviation, whereas the -1g aeroelastic analysis is a better basis to represent and design the wing-strut interaction and account for the buckling of the strut. All optimizations are performed using Altair Optistruct [24].

3.4 Moveable sizing

The stream aims at designing a suitable trailing edge control surface layout to capitalize on the increased design space and opportunities pertinent to a dry wing configuration; and to facilitate multi-objective control of the wing in terms of handling qualities, high-lift requirements, drag minimization, and load alleviation (manoeuvre and gust).

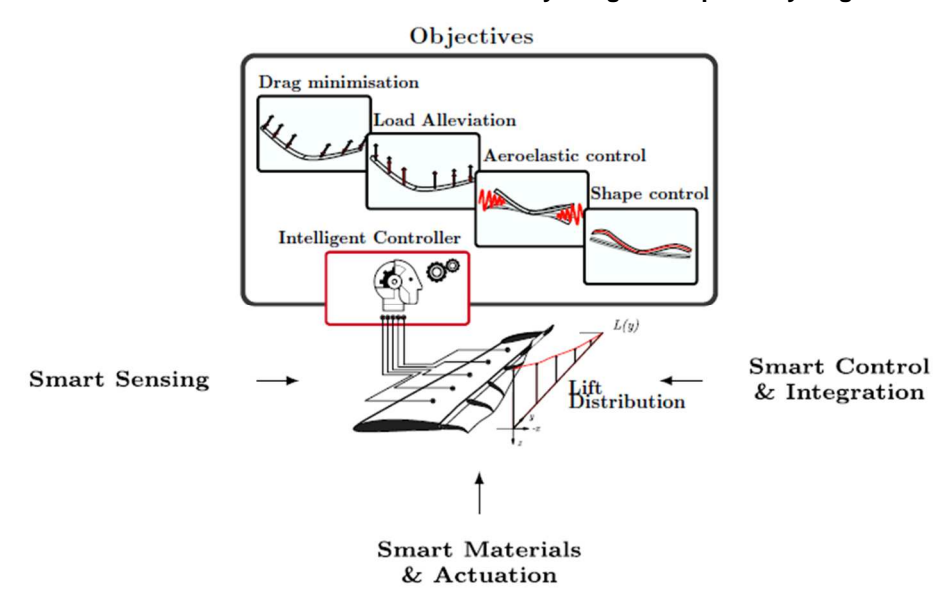


Figure 14 - Design approach for multifunctional movables.

3.4.1 L0: Empirical formulations

The FAST-OAD software doesn't really implement control surface design, as its handling quality module is based on the sizing of the tail surfaces and wing area to satisfy stability and control requirements:

- The wing area is sized upon the approach speed requirements, under flapped configuration at landing. C_{Lmax} is evaluated with empirical formulas relying on the fraction of span covered by high-lift devices, and the chord fraction of flaps and slats,
- The horizontal tail is sized upon the take-off rotation requirement, and looped with the wing
 position to ensure a suitable static margin,
- The vertical tail ensures en-route lateral stability and one-engine-out control requirement.

Therefore, at L0 level, the movables capabilities for load alleviation or dynamic behaviour estimation are not taken into account.

3.4.2 L1: Doublet Lattice Method Aerodynamics

The doublet lattice method (DLM) is used to model the movables aerodynamics. Using the approach from de Boer et al. [25], the aerodynamic force which is generated by the movables is modelled using the downwash distribution in the continuous space. A brief overview of the used formulation is presented here. Inside the DLM formulation, the movable aerodynamics can be modelled using the following [26][27].

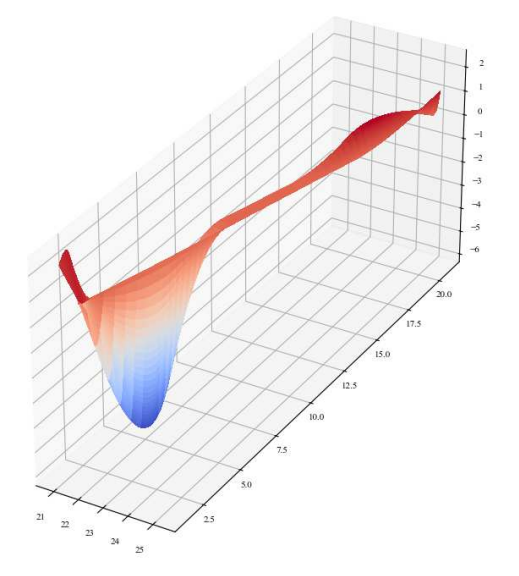
$$\mathbf{P}_{k}^{\mathsf{a, cs}} = q_{\infty} \mathbf{S}_{kj} \mathbf{AIC} \, \mathbf{w}_{j, \, \mathbf{cs}} \tag{1}$$

Using the same panel discretisation, the aerodynamic integration matrix \mathbf{S}_{kj} and the AIC matrix **AIC** are kept constant, meaning that the main driver behind the movable aerodynamics is the movable downwash $\mathbf{w}_{j,\,\mathrm{cs}}$.

Inside the parameterisation presented by de Boer et al. [25], the downwash $\mathbf{w}_{j,\,\mathrm{cs}}$ is modelled in the continuous space using a B-spline surface, with an example surface shown in Figure 15. The application of the downwash distribution requires a control point grid, with an example grid shown in Figure 16, with the spanwise and chordwise fractions of the region which is influenced by the continuous parameterisation remaining constant for all configurations which are analysed. Even though Figure 16 shows 4 chordwise control points, in this case all chordwise control points will have the same downwash value assigned to them, with the spanwise downwash value allowed to vary.

The optimisation problem for the movable parameterisation is the following:

$$\min_{\mathbf{D}_{CP}}(V_i)$$
 s.t. $C_1 \dots C_4$ are satisfied. (2)



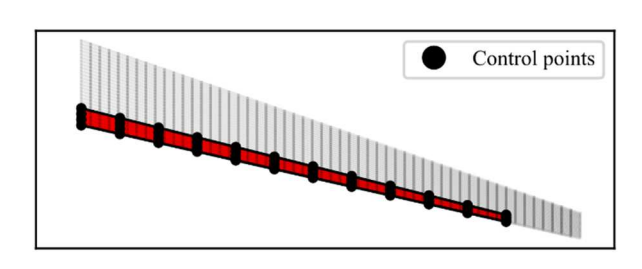


Figure 16 - Movable regions influenced by continuous parameterisation.

Figure 15 - Moveable sizing - B-spline surface.

where the design variables \mathbf{D}_{CP} are the downwash levels at the control points, V_i the objective functions and C_i the constraints. The objective considered during the optimisation process, is the minimisation of the bending moments inside the wing

$$V_1 = M_{x,c} \tag{3}$$

where the subscript c indicates the location of interest, which are the wing root and the wing-strut intersection, as indicated in Figure 3. The first constraint used is:

$$C_1: \mathbf{P}_{c, lower} \le \mathbf{P}_{c} \le \mathbf{P}_{c, upper}$$
 (4)

which is the limit load constraint, that is necessary to make sure that the aircraft structure is not overstressed when the lift is redistributed over the wing. A detailed description of the manoeuvres used to determine the limit loads is given in 27[25].

The purpose of the second constraint

$$C_2: \begin{cases} -0.3 \le w_j^{CP} \le 0.3 \\ -15^{\circ} \le \eta \le 15^{\circ} \end{cases}$$
 (5)

is to make sure that the deflections of the movables do not reach values which cannot be modelled using the DLM method, as the DLM method does not account for the occurrence of flow separation. The limits for the deflection angles are determined as if the continuous region behaves as a conventional movable and are expressed in downwash level, with equivalent deflection angles being $\pm 20^\circ$. The \mathcal{C}_2 constraints also adds a constraint to the elevator deflection angle η , as the aircraft needs to be trimmed during the application of the downwash distribution, with the limits of the elevator deflection angle ranging between $\pm 15^\circ$.

The third constraint

$$C_3: p \ge 15^{\circ}/s \tag{6}$$

is the handling quality constraint, which is included as a steady-state roll rate which must be achievable by the aircraft. The required steady-state roll-rate of 15 °/s can be derived from the roll performance requirements stated in CS25 [27].

The final constraint

$$C_4: -10^\circ \le AoA \le 10^\circ \tag{7}$$

is necessary because the DLM method used to model the aerodynamics inside the Level 1 movable sizing module does not consider flow separation.

The optimisation of the downwash distribution for a minimisation of the root bending moment redistributes the load, with Figure 17 showing the optimised downwash and corresponding lift distribution for a 2.5g pull-up manoeuvre using the U-HARWARD aircraft model. The results from de Boer et al. [25] show that the using the movables allowed for a 41% reduction of the root bending

moment when compared to a clean wing subjected to the same load case.

By evaluating the different wing planforms and structures obtained in LEVEL8 OAD output, the achievable manoeuvre load alleviation performance can be determined by applying the presented approach and optimisation problem.

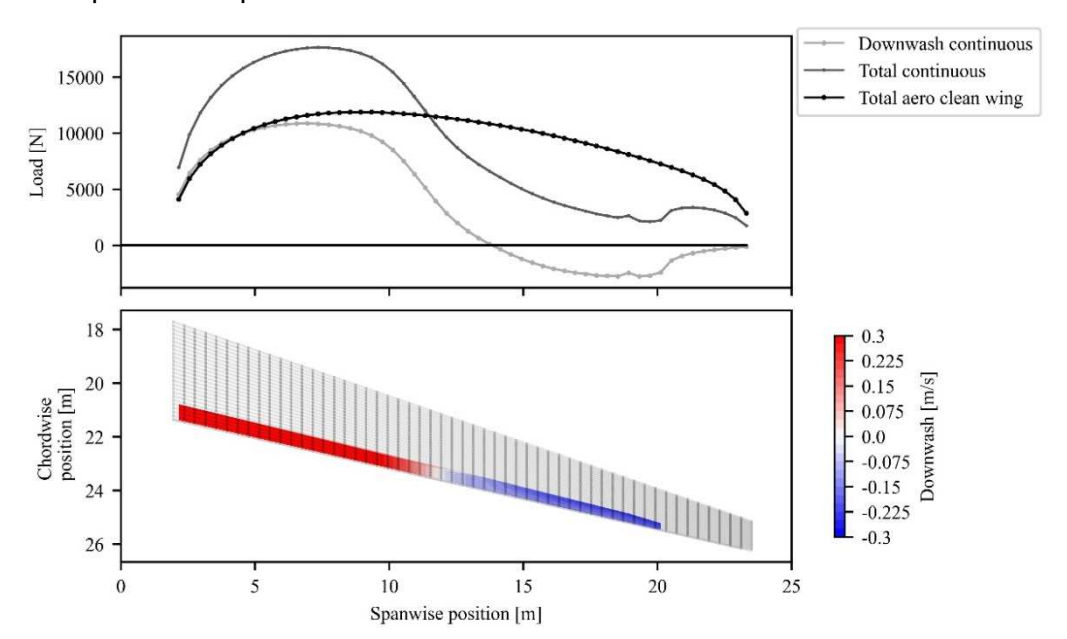


Figure 17 - Lift and downwash distribution for $min(M_x)$ at the wing-root for the U-HARWARD planform [25]

4. Exploration of the design space

Based on the DoE detailed in Table 1 and Figure 3, as well as the results obtained after the initial OAD sizing loops (see 2nd step in §2.2), a detailed analysis of these results is proposed in the following section as well as an overview of the first high-fidelity results obtained for aerodynamics and structural sizing (see 3rd step in §2.2). This analysis aims at providing an overview of the design space with a sensitivity analysis of the main functions of interest (fuel weight, LoD in cruise, MTOW, OWE, wing and strut weights) with respect to the different design variables and at identifying the key SBDW design drivers.

4.1 Initial sizing with low-fidelity methods (L0)

In this section, the results are only based on low-fidelity methods and the performances of the SBDW concept are compared with a classical cantilever wing configuration. The same low-fidelity process with few adaptations (removal of the strut, low wing) has been used to have comparable results. For the cantilever wing, the same design variables as those presented in Table 1 have been defined (without considering the strut design variables). It is worth reminding that for each point of the DoE (i.e. each combination of design variables) a full aircraft sizing is performed, which means that all the lifting areas and all the weights are recomputed to ensure that the design range is achieved. In order to analyse the results on the complete design space, surrogate models have been generated from the full DoE (1280 configurations) using the SMT toolbox [3] for all functions of interest.

Performance of the SBDW concept

Figure 18 shows the Block Fuel weight (LH_2) for the design mission with respect to the wing Aspect Ratio and the Wing / Strut junction for two values of the LAF factor (LAF=0.0 - without load alleviation, and LAF=0.3 - with a quite aggressive load alleviation strategy). The values for all other design variables are fixed. In both cases, the design space shows a clear minimum. Without load alleviation (LAF=0.0), the optimal wing Aspect Ratio is about 24 with a Wing / Strut junction located at mid span wing. With the activation of the load alleviation system, the optimal wing Aspect Ratio (AR) increases (up to 25.5) and the optimal Wing / Strut junction location is moving towards the inner wing. This result can be easily explained: with a smart load alleviation strategy, the sizing loads (and in particular the wing root bending moment) are reduced which enables to further increase the wing Aspect Ratio and to reduce the length of the strut as the loads on the external

wing are partially alleviated for the sizing cases (the corresponding centre of lift is moving towards the inner wing).

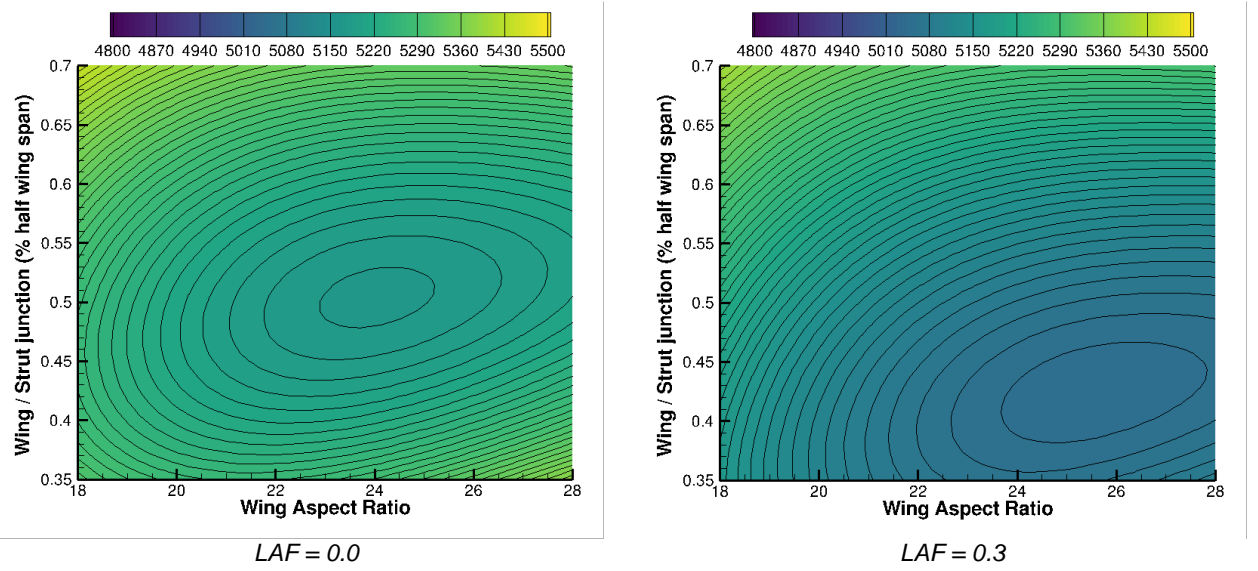


Figure 18 - Mission Block Fuel Weight of the SBDW concept wrt Wing Aspect Ratio and Wing / Strut junction for two LAF values.

Figure 19 shows the MTOW in the same part of the design space (with respect to the wing AR and the Wing / Strut junction for two values of the LAF factor). For all Wing ARs and for both LAF values, the MTOW shows a clear minimum, which is almost at a constant Wing /Strut junction location value. This value is about 0.6 without Load Alleviation and slightly increases with wing AR (up to 0.63 for AR=28), with the aggressive LAF value, this optimal value is lower (0.58) as explained before and do not evolves with wing AR. This evolution of the MTOW is perfectly aligned with the trends observed for the OWE (Figure 20) and the Wing/Strut Weight (Figure 21).

In terms of aerodynamics, the expected trends are observed. For a given Wing /Strut junction location, the cruise LoD increases with the wing AR by about 8% with a long strut between 18 and 28 and by about 15% for short struts. This underlines the non-negligible effects of the strut on the aerodynamic performance as in this first design scenario the strut is non-lifting and thus represents only an additional source of friction drag in terms of aerodynamics. The difference between a long (with a Wing / Strut junction value of 0.70) and a short (with a Wing / Strut junction value of 0.35) is about 7% for a wing AR of 18 and 13% for a wing AR of 28. These trends do not depend on the LAF value, only the absolute cruise LoD value is affected by snow-ball effects: with a load alleviation system, the weight of the aircraft is reduced as the wing area but all other aircraft elements remain almost constant which increases the contribution of the non-lifting elements to the drag and thus causes a decrease of the cruise LoD.

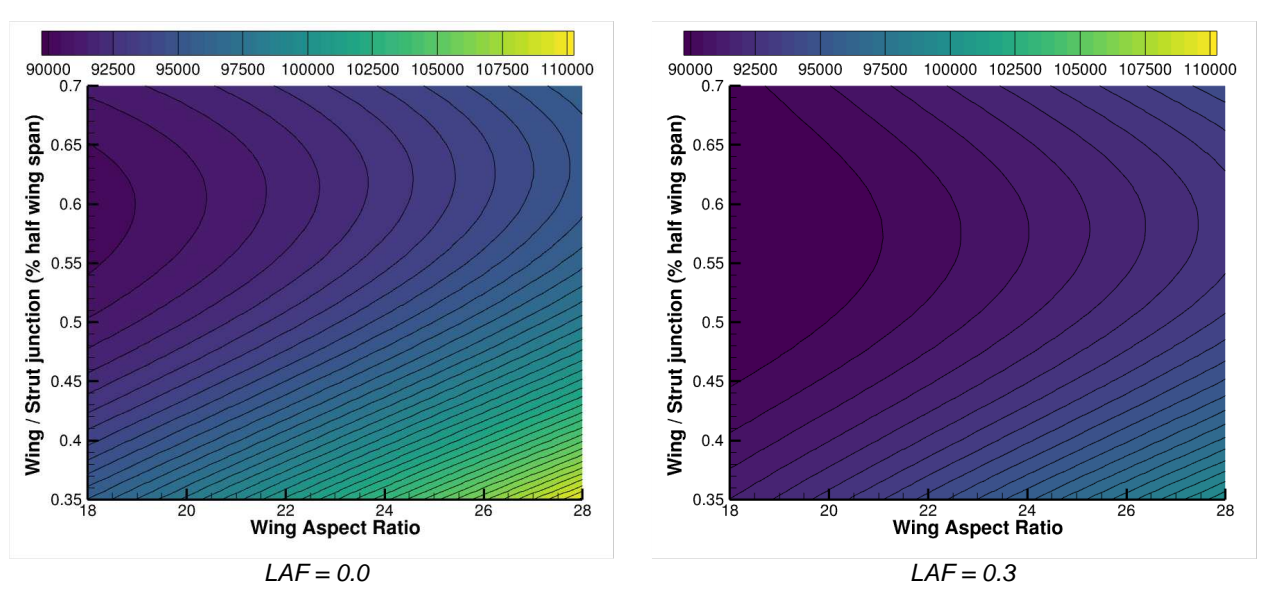


Figure 19 - MTOW of the SBDW concept wrt. Wing Aspect Ratio and Wing / Strut junction for two LAF values.

Strut-Braced Dry Wing Concept for Hydrogen-Powered Aircraft

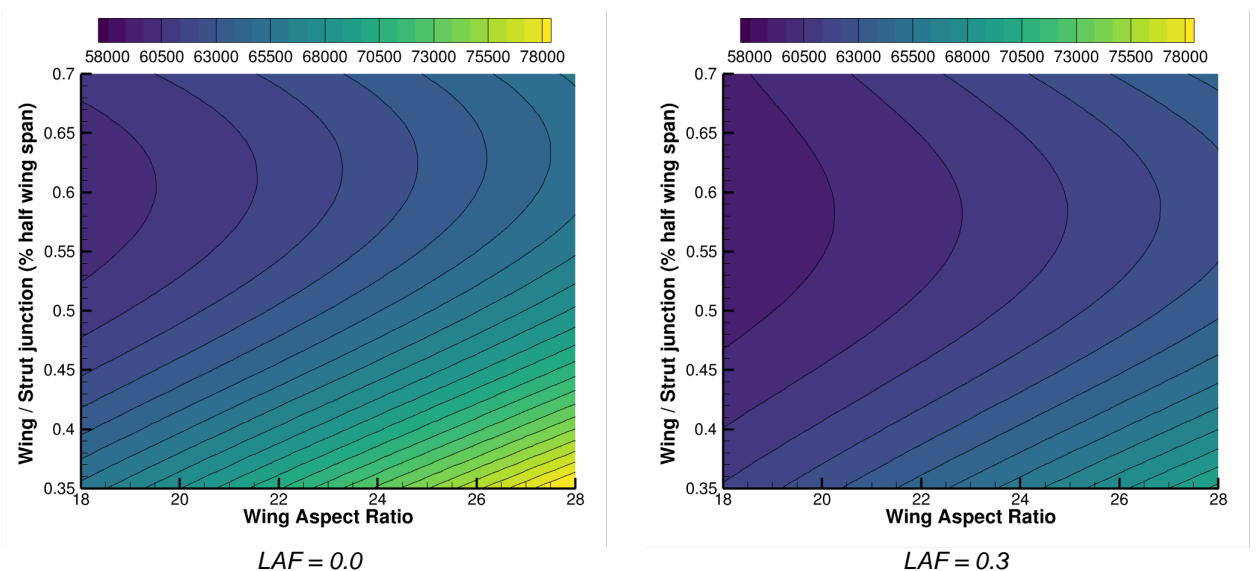


Figure 20 - OWE of the SBDW concept wrt. Wing Aspect Ratio and Wing / Strut junction for two LAF values.

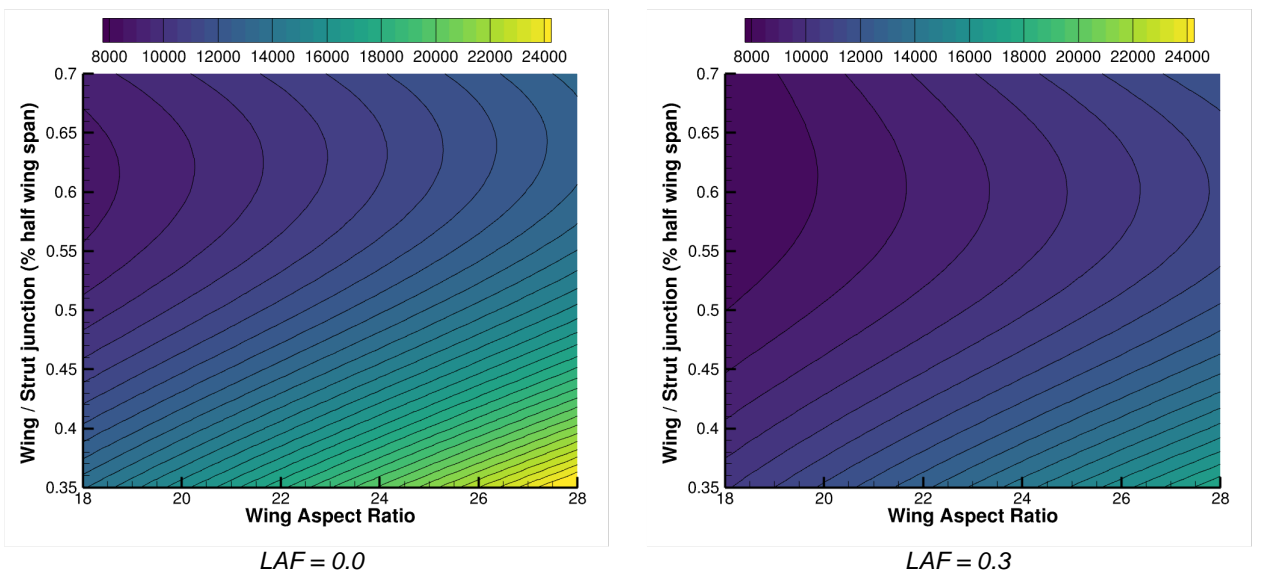


Figure 21 - Wing/Strut weight of the SBDW concept wrt. Wing Aspect Ratio and Wing / Strut junction for two LAF values.

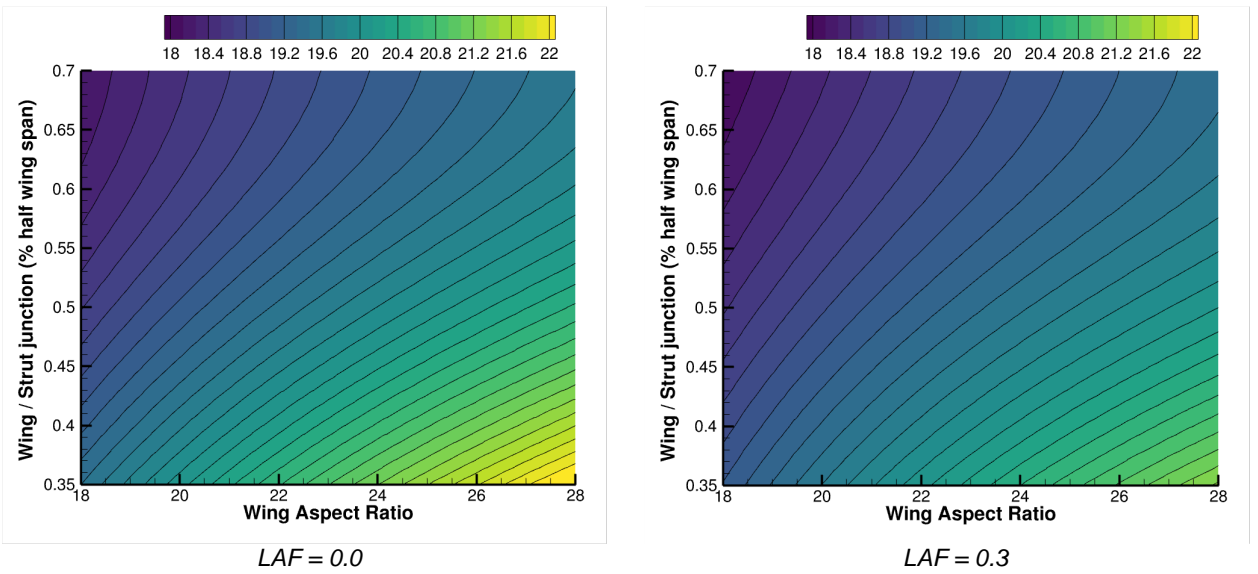


Figure 22 - Cruise LoD of the SBDW concept wrt. Wing Aspect Ratio and Wing / Strut junction for two LAF values.

Performance of the Cantilever concept

In order to compare the performance of the SBDW concept, the same exercise has been achieved on a cantilever wing configuration. The range for the wing AR has been increased (from 10 to 28) in order to include in the design space the values of the current aircraft. The results show as a high dependency to the wing AR but the Block Fuel sensitivities wrt. Relative Kink location are rather small for both LAF values. With respect to the wing AR, the Mission Block Weight shows a clear minimum in both cases and the optimal wing AR value increases with the LAF factor as expected as for the SBDW configuration. For LAF=0.0, the optimal wing AR value is about 16 whereas with the very aggressive LAF value the optimal wing AR is about 19. It can be noticed that this value are rather high but can be partly explained by the properties of the black aluminium material.

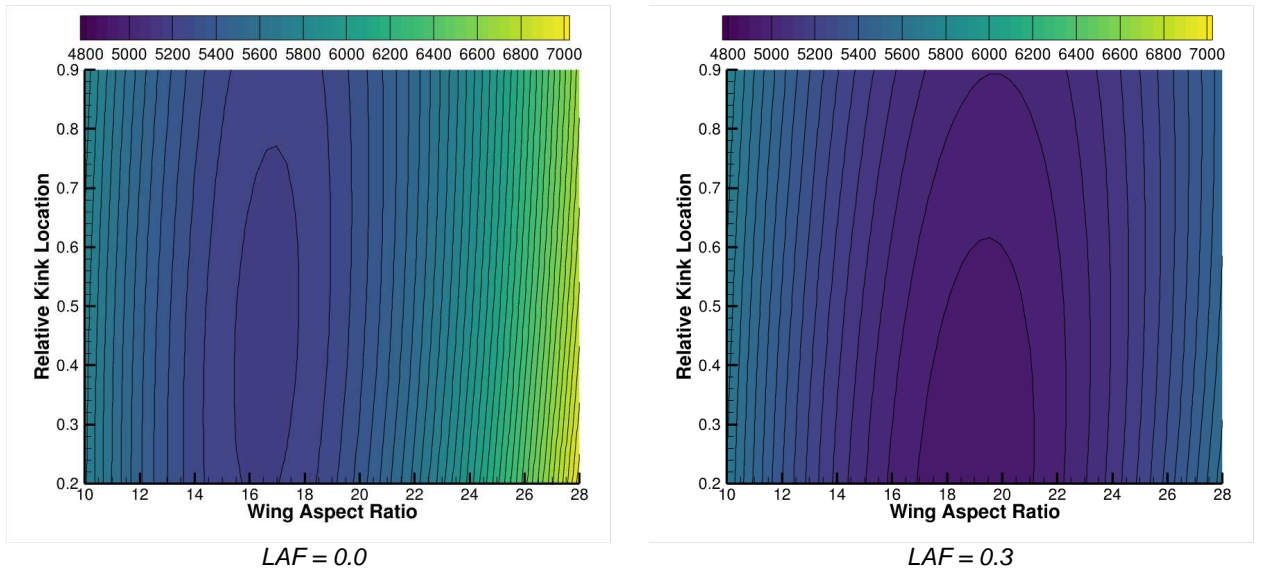


Figure 23 - Mission Block Fuel Weight of the Cantilever configuration wrt. Wing Aspect Ratio and Kink Spanwise Location for two LAF values.

SBDW Concept vs Cantilever configuration - Synthesis

In order to complement the exploration of the design space but also understand the impact of advanced technologies on the performance of the LH₂ cantilever wing and SBDW concepts, the same design procedure was applied with a more conventional aluminium material.

The results are synthetized in Figure 24 which shows the evolution of the Mission Block Fuel Weight with respect to the Wing AR for the 8 configuration (Cantilever and SBDW, Aluminium and Black Aluminium, Without and without aggressive Load alleviation). For each Wing Aspect Ratio, the other variables (especially the strut variables) are set to constant values. It clearly underlines that both technologies (load alleviation and material) affect more the Cantilever configurations than the SBDW concept which is not very sensitive to these effects. This is clearly visible when considering the minimum Block Fuel configurations.

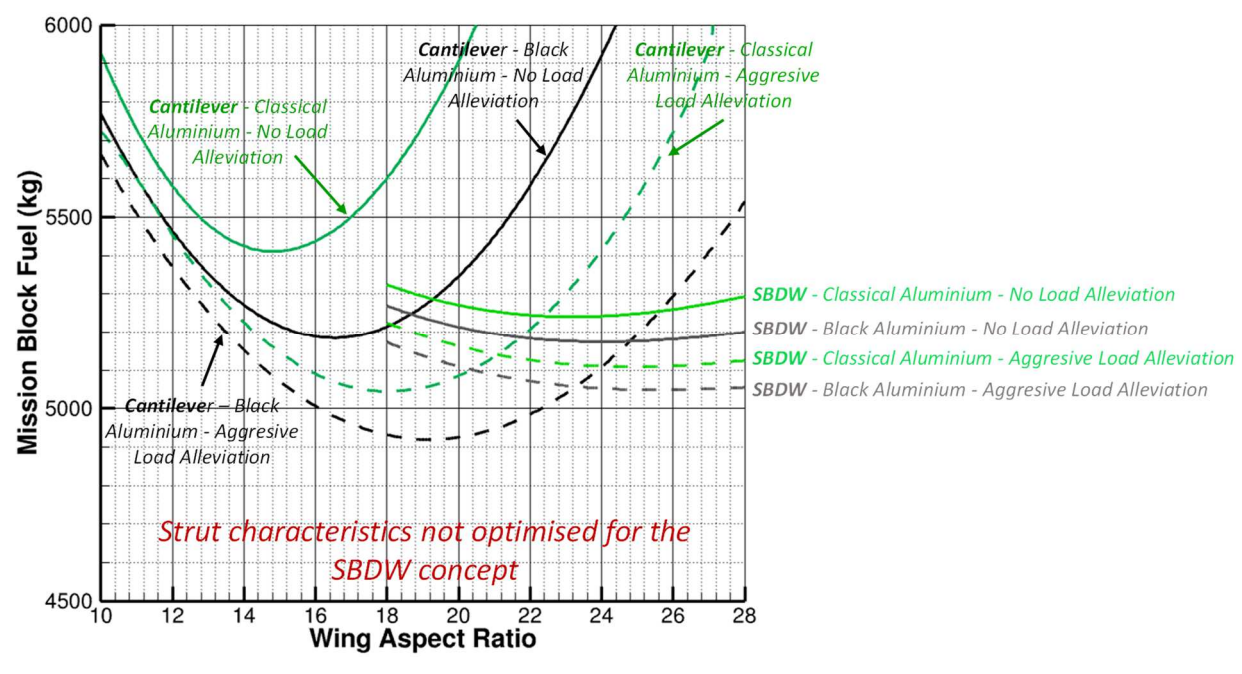


Figure 24 - Mission Block Fuel Weight wrt. Wing Aspect Ratio for the LH2 cantilever wing and SBDW concepts for a classical and a black aluminium for two LAF values.

Impact of Load Alleviation

Table 2 shows the impact of the aggressive load alleviation strategy (wrt. to no load alleviation strategy) on different functions of interest. The optimal wing AR strongly increases for the Cantilever configuration by 20% and 15% respectively with the classical and black aluminium. The increase reaches only respectively 7% and 8% for the SBDW concepts. In terms of Block Fuel, the impact is between 5 and 6.8% for the Cantilever configuration, it is only about 2.5% for the SBDW concept. As far as weights are concerned, the decrease of the MTOW is about 3% for the Cantilever configuration, and about 0.5% for the SBDW configuration. In terms of OWE and Wing Weight (+ strut weight for the SBDW), the impact of the load alleviation system is very important for the cantilever configuration (-3.6% for the OWE and between -7.9% and -9.6% for the Wing Weight) but very limited for the SBDW (about -0.6% for the OWE and about -0.9% for the Wing / Strut Weight). In terms of LoD, the increase is mainly due to the increment of the optimal AR for all configurations. The benefits are between 3% and 5% for the Cantilever configurations, and about 2% for the SBDW concept.

Impact of Load Alleviation (LAF=0.3 -	Cant	ilever	SBDW		
LAF=0.0)/LAF=0.0	Alu	Black Alu	Alu	Black Alu	
AR	20.6%	15.7%	6.9%	8.3%	
Block Fuel	-6.8%	-5.1%	-2.48%	-2.4%	
MTOW	-2.9%	-2.8%	-0.6%	-0.5%	
OWE	-3.6%	-3.7%	-0.7%	-0.5%	
Wing (+Strut) Weight	-7.9%	-9.6%	-1.0%	-0.8%	
Cruise LoD	5.2%	3.1%	2.1%	2.2%	

Table 2 - Impact of aggressive Load Alleviation strategy on Aircraft performance (Relative differences: (LAF=0.3 - LAF=0.0)/LAF=0.0).

Impact of Material

Table 3 shows the impact of the material (Black Aluminium vs Aluminium) on the performance. The increase of the optimal AR is as expected more important for the Cantilever configurations (respectively 10% and 5.6% without and with load alleviation strategy) against 3% and 4% for the SBDW concept. In terms of Block Fuel, the benefits are respectively about 4% and 2.5% for the cantilever configuration but only 1.2% for the SBDW concept. For the different weights, the trends are the same (-2% in terms of MTOW for the Cantilever configuration vs -0.7% for the SBDW

concept, about -2.6% vs -1% in terms of OWE and between -5.5% to -7.3% vs -3.6% for the wing (+strut) weight. In terms of cruise LoD, again the increase is due to the augmentation of the optimal wing AR.

Impact of Material (Black Alu - Alu)/Alu)	Cantilever – No load alleviation	Cantilever – Aggressive load alleviation	SBDW – No load Alleviation	SBDW – Aggressive load Alleviation
AR	10.1%	5.6%	2.7%	4.0%
Block Fuel	-4.2%	-2.5%	-1.2%	-1.2%
MTOW	-2.0%	-2.0%	-0.7%	-0.6%
OWE	-2.8%	-2.6%	-1.0%	-0.9%
Wing (+Strut) Weight	-5.5%	-7.3%	-3.7%	-3.5%
Cruise LoD	2.7%	0.7%	0.6%	0.6%

Table 3 - Impact of the material on Aircraft performance (Relative differences: (Black Aluminium - Aluminium)/Aluminium).

Comparison vs Reference aircraft

To give more insights on the potential of all these configurations with respect to a more conventional aircraft configuration with 2020's technology assumptions, the performance of all optimal concepts are compared to the Cantilever wing configuration designed using classical aluminium, a wing AR of 10 and no aggressive load alleviation strategy.

In terms of optimal wing AR, the increase is huge compared to the reference aircraft for both concepts but as expected even more pronounced for the SBDW concepts where the optimal values are between 23 and 26. For the cantilever configuration, the optimal values are between 15 and 19. As far as the Mission Block Fuel Weight is concerned, the benefits strongly increase with the use of advanced technologies. Without Load alleviation and the use of classical aluminium, the benefits for the Cantilever configuration are about 8.7% against 11.6% for the SBDW concept. As the cantilever configurations are more sensitive to the use of the advanced technologies, the difference of benefits between the two concepts progressively decreases with the integration of these technologies. With the use of black aluminium but without aggressive load alleviation strategy, both configurations have similar performance in terms of Mission Block Fuel Weight with a benefit of about 12.5% compared to the reference. With the use of the aggressive load alleviation system (with classical aluminium), the performance of the optimal cantilever configuration is slightly better than the one of the SBDW with a benefit compared to the reference of about 15% against 14% for the SBDW concept. When considering both advanced technologies, the difference between both configurations is even more in favour of the cantilever concepts with a benefit of about 17% vs 15% for the SBDW concept.

This very good performance of the cantilever wing configuration in terms of Block Fuel was obtained at a price of a considerable weight increase unlike the SBDW concepts which enables to obtain lighter configurations. Indeed with the cantilever configurations, the MTOW increase is between 2% and 7% compared to the reference configuration whereas for the SBDW configuration a decrease of 3% to 4% is observed. For the OWE, the trend is even more pronounced with values between 4% and 11% for the cantilever configurations against a decrease of 3% to 5% for the SBDW configurations. Most of these differences are due to wing weight increase: between 29% and 51% for the cantilever configurations compared to the reference aircraft against a decrease of 5% to 9% for the SBDW configurations.

The benefits of the SBDW concept in terms of weight are obvious but they are counterbalanced by some penalties in cruise LoD which explained the results observed for the Mission Block Fuel Weight. Compared to the reference aircraft, as expected all configurations provide an important step forward due to the significant wing AR increase. For the cantilever configurations, the benefits are between 20% and 27% depending on the optimal wing AR, there are between 14% and 17% for the SBDW. Even with larger wing AR, the SBDW concepts do not provide additional aerodynamic benefits compared to the cantilever configuration. The benefits on the induced drag thanks to the high wing AR values are counterbalanced by the presence of the strut which is responsible for additional sources of friction drag.

One cannot forget that all these results were obtained without any optimisation of the strut

and that potential additional benefits for the SBDW concepts could be obtained by exploring more widely the design space and especially the strut design parameters. Additionally the opportunity to have a lifting strut would need to be analysed in details. These results are not presented in the paper but will be available during the next steps of the projects. And finally, these results are obtained with low-fidelity methods, especially for the structural sizing. This might lead to optimistic results in particular for the cantilever configuration where dynamic effects such as flutter limits are not considered. The study will then be continued with a multi-fidelity approach which might lead to different conclusions.

Delta vs REFERENCE (%)	Cantilever – No load alleviation		Cantilever – Aggressive load alleviation		SBDW – No load Alleviation		SBDW – Aggressive load Alleviation	
	Alu	Black Alu	Alu	Black Alu	Alu	Black Alu	Alu	Black Alu
Wing AR	49.2%	64.2%	80.0%	90.0%	133.8%	140.0%	150.0%	160.0%
Block Fuel	-8.7%	-12.5%	-14.9%	-17.0%	-11.6%	-12.7%	-13.8%	-14.8%
MTOW	6.9%	4.7%	3.7%	1.7%	-2.8%	-3.5%	-3.4%	-4.0%
OWE	10.8%	7.9%	6.8%	4.0%	-3.0%	-4.0%	-3.6%	-4.5%
Wing (+Strut) Weight	50.6%	42.3%	38.8%	28.6%	-5.0%	-8.5%	-5.9%	-9.2%
Cruise LoD	19.6%	22.8%	25.7%	26.6%	13.9%	14.5%	16.3%	17.0%

Table 4 - Performance wrt to the reference cantilever configuration (Aluminium, No Load Alleviation, Wing AR=10).

4.2 High-fidelity analysis (L0 to L3)

In this section a first description of the high-fidelity results obtained for the aerodynamics and structural sizing is proposed.

4.2.1 Aerodynamics

To build the multi-fidelity RSM for aerodynamics, EULER and RANS simulations were performed as described in $\S 0$ (80 EULER simulations and 20 for RANS). The use of the Far-field drag methods enables the evaluation of the different physical drag components. The results obtained for the last 20 configurations of the DoE are plotted in Figure 25 for the cruise C_L (0.65). These values correspond only to the Wing /Strut /Fuselage configurations as all other aircraft components were not considered in the EULER and RANS simulations. Note that the L0 drag of these additional elements are added to the L1 and L2 drag values to evaluate the total drag of each configuration at OAD level. For the EULER simulations, the friction and viscous pressure drag coefficients are also evaluated using the L0 method. In Figure 25, the induced and wave drag components are plotted for both EULER and RANS simulations, the viscous pressure, friction and total drag coefficients are represented only for the RANS computations.

The comparison between the L1 (EULER) and L2 (RANS) results highlights that similar trends are captured by both methods when comparing the different configurations for the induced and wave drag components. As expected, an overestimation of the wave drag is observed with the EULER simulations but to counterbalance the evaluation of the total drag a slight underestimation of the induced drag is observed with these EULER simulations. The fact of having similar trends between the different levels of fidelity will ensure the definition of robust and accurate RSMs for aerodynamics.

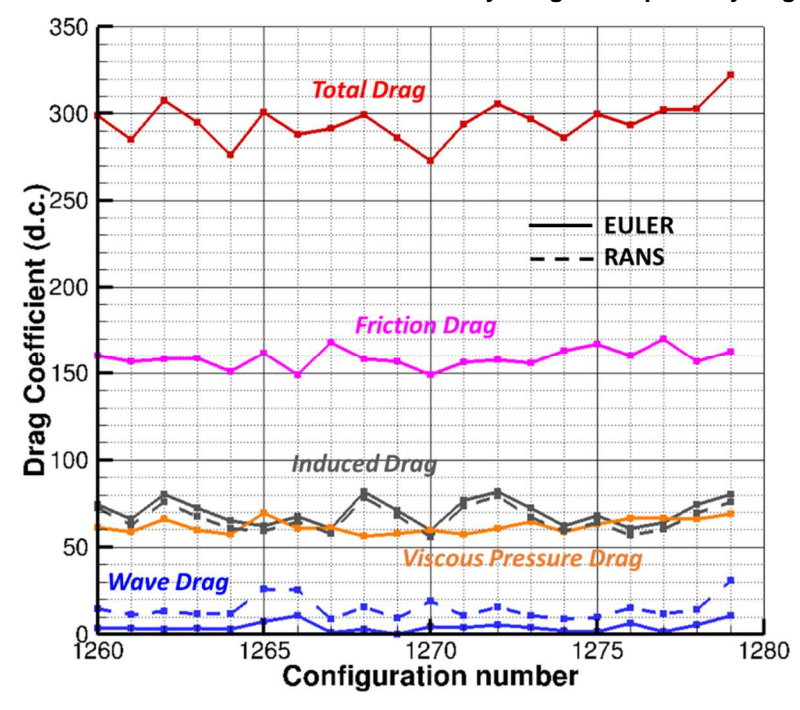


Figure 25 - Drag Coefficients from EULER and RANS simulations for the last 20 configurations of the DoE (in d.c. = 1 10⁻⁴).

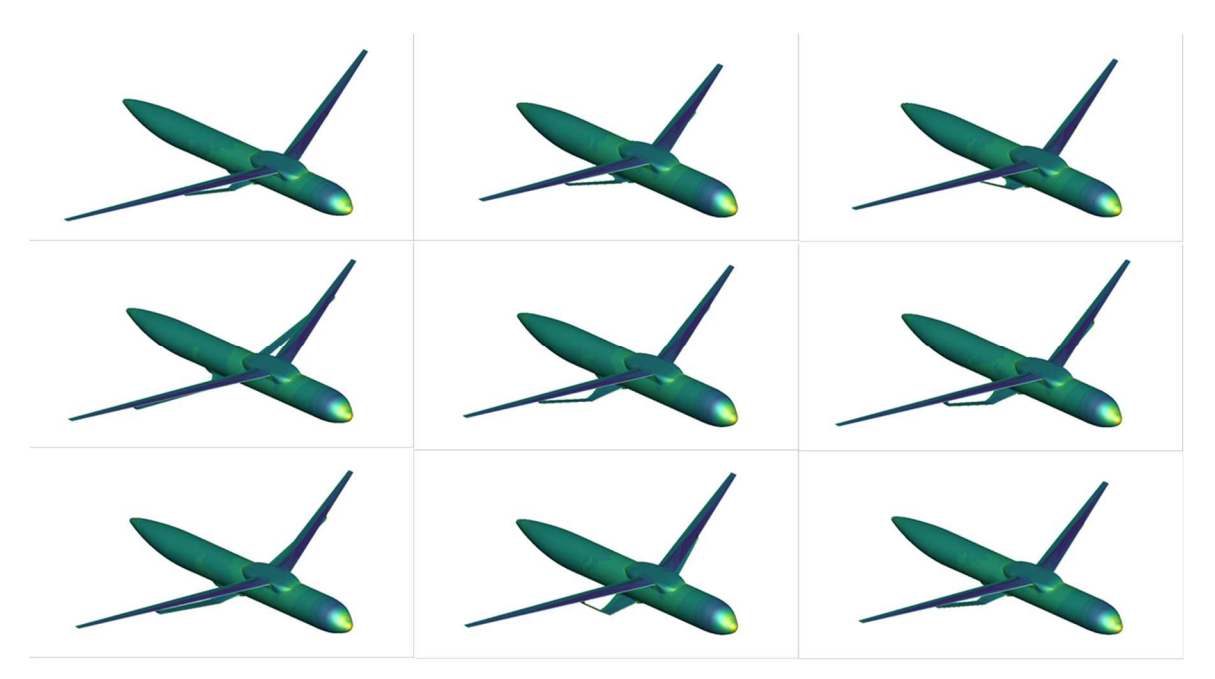


Figure 26 - Pressure distributions from the RANS simulations for 9 of the last 10 configurations of the DoE.

4.2.2 Structural sizing

In this section, first results coming from the L1 module for the structural sizing are presented. More details can be found in [20].

Figure 27 shows the evaluation and Wing / Strut Weight wrt. the Wing Aspect Ratio as well as Wing / Strut junction location for both L0 and L1 modules. The trends between both fidelities are similar with an optimal Wing / Strut junction value almost independent of the Wing AR but these optimal values are significantly different (about 0.65 for L0, about 0.45 for L1). In terms of absolute values, the L1 mass is slightly lower than the results of the L0 module especially for very high Wing AR and low and Wing / Strut junction values. These results will be exploited in the next steps of the study which may affects the overall performance and aero-structural compromises of the optimal SBDW configurations.

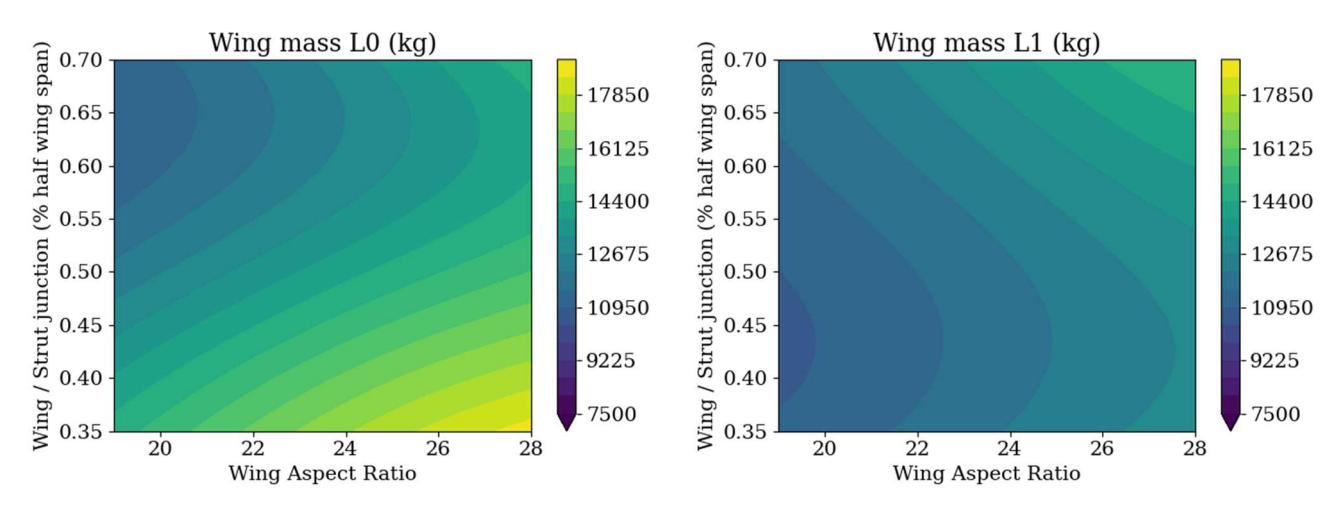


Figure 27 - Wing/Strut weight of the SBDW concept wrt. Wing Aspect Ratio and Wing / Strut junction for the L0 and L1 structural sizing modules (Black Aluminium, LAF=0.0).

Figure 28 shows some examples among the DoE of wing and strut deformations of the Finite Element Model under 2.5g loads. Significant differences can be observed especially when the length of the strut increases.

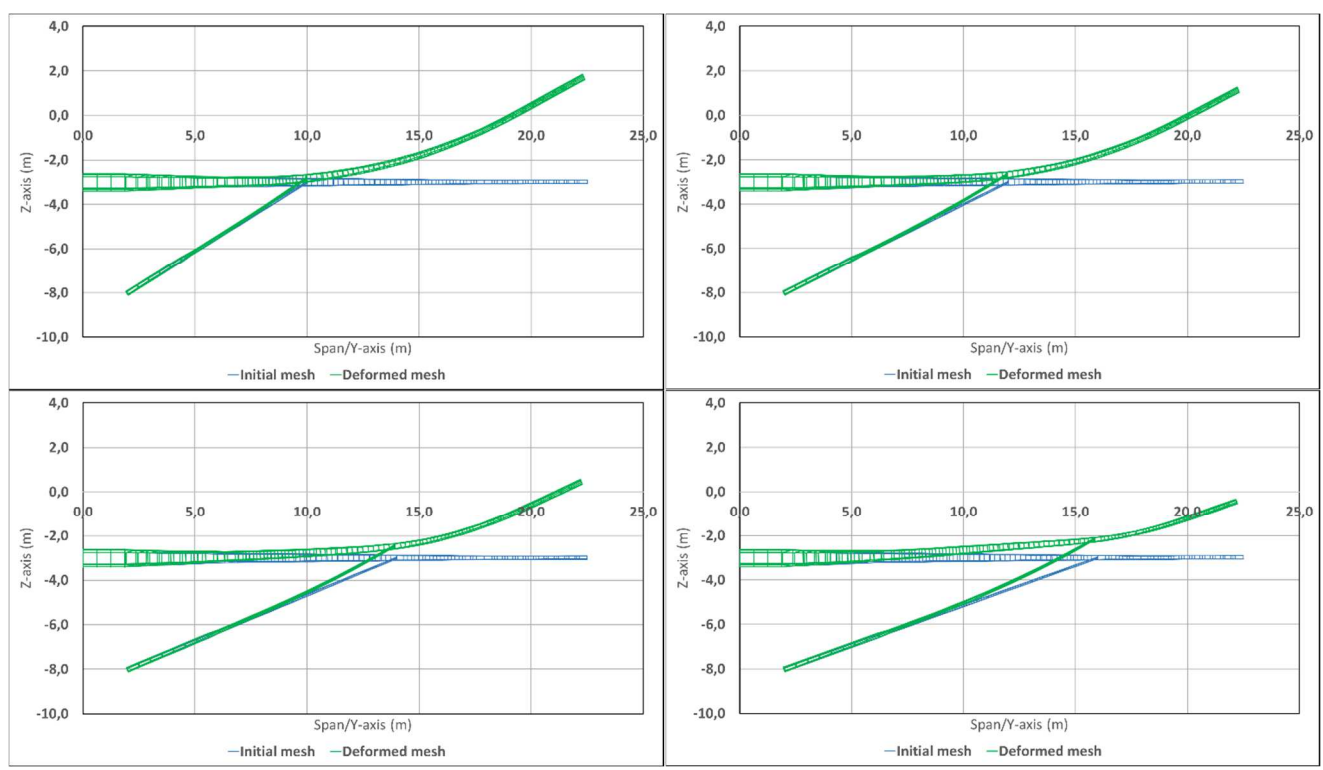


Figure 28 - Examples of wing /strut deformations in the case of 2.5g load case (L1 module) [20].

5. Conclusions and perspectives

This paper describes the overall design approach set-up within the Clean Aviation UPWING project by ONERA, Technical University of Delft and University of Stuttgart to design and analyse the potential of the Strut-Braced Dry Wing Concept powered by LH₂ engines. An original multi-fidelity and multi-disciplinary approach is presented and has been implemented in this context. All disciplinary modules as well as the coupling strategies are detailed in the first part of the paper. To widely explore the design space of the SBDW concept, a dedicated parameterization is proposed together with the definition of a specific parameter to model the impact of advanced load alleviation strategies as well as a so called 'black aluminium' fictitious material for the structural sizing of an equivalent isotropic wing and the strut.

In the second part of the paper, first results on the SBDW concept using the complete L0 process are presented and compared with the more conventional Cantilever configuration. The impact of

advanced technologies such as smart load alleviation strategy and advanced material are also proposed. The results underlines that the SDBW concept is less sensitive than the Cantilever configuration to technology effects and that the conclusions in terms of Mission Fuel Weight strongly depend on the technology level assumptions. With current technologies, the SDBW concept provides an additional benefits of 3% compared to the optimal Cantilever configuration but with the use of both advanced technologies (aggressive Load Alleviation strategy and Black Aluminium), the Cantilever configuration exhibits 2% of additional benefits compared to the SBDW concept. Compared to the reference configuration (Cantilever Wing configuration with a Wing AR of 10 and the use of current technologies), the maximum benefits are about 17% for the Cantilever configuration and 15% for the SBDW concept. It is essential to note that these results for the optimal Cantilever configuration were obtained at a price of a significant weight increase (MTOW, OWE and Wing Weight) whereas for the SDBW concept lighter configurations are obtained. *Moreover, in this* first analysis of the results, the strut characteristics are not optimized which could lead to additional benefits for the SBDW concept (including the possibility to have a lifting strut). Additionally, design very efficient Cantilever aircraft configurations imposes the use of advanced technologies such as aggressive Load Alleviation Strategy, which may be difficult to certify. For instance, to alleviate the loads during critical gusts, advanced optical technologies such as the LIDAR are required but their certification for civil aircraft remains a challenge. On the contrary, the performance of the SBDW concept is less dependent of the maturity of these technologies, which may be an advantage for future civil aircraft program.

It is to be noted that these results were obtained with an aircraft sizing process using for the moment only low-fidelity models. In the next steps of the Clean Aviation UPWING project, the results of all high-fidelity disciplinary modules will be exploited through the integration of accurate Surrogate Models in the Overall Aircraft Design process. This will enable to complete the current analysis and explore more widely the design space and especially the degree of freedom offered by the strut. Moreover, the disciplinary tools will be enhanced to:

- Consider more critical sizing cases for the structural wing and strut design,
- Fully explore the design space offered by the dry-wing concept (topology optimisation of the wing and strut structure, resizing of the movable layout)
- Account for the aero-propulsive interactions between the engine (UHBR or USF) and the Wing / Strut as well as the aero-elastic properties of the SBDW and Cantilever configurations.

6. Acknowledgement

The project Ultra Performance Wing (UP Wing, project number: 101101974) and ACAP (project number: 101101955) are supported by the Clean Aviation Joint Undertaking and its members. co-Funded by the European Union. Views and opinions expressed are however those of the author(s) only and do not necessarily reflect those of the European Union or Clean Aviation Joint Undertaking. Neither the European Union nor the granting authority can be held responsible for them.



7. Contact Author Email Address

michael.meheut@onera.fr

8. Copyright Statement

The authors confirm that they, and/or their company or organization, hold copyright on all of the original material included in this paper. The authors also confirm that they have obtained permission, from the copyright holder of any third party material included in this paper, to publish it as part of their paper. The authors confirm that they give permission, or have obtained permission from the copyright holder of this paper, for the publication and distribution of this paper as part of the ICAS proceedings or as individual off-prints from the proceedings.

References

- [1] G. Carrier and al. "Multidisciplinary analysis and design of strut-braced wing concept for medium range aircraft". AIAA Scitech January 2022. 10.2514/6.2022-0726.
- [2] David, C., Delbecq, S., Defoort, S., Schmollgruber, P., Benard, E., & Pommier-Budinger, V. (2021). From FAST to FAST-OAD: An open source framework for rapid Overall Aircraft Design. In IOP Conference Series: Materials Science and Engineering (Vol. 1024, No. 1, p. 012062). IOP Publishing.
- [3] https://smt.readthedocs.io/en/latest/index.html
- [4] Charayron, R., Lefebvre, T., Bartoli, N., & Morlier, J. (2023). Towards a multi-fidelity & multi-objective Bayesian optimization efficient algorithm. *Aerospace Science and Technology*, *14*2, 108673.
- [5] Defoort S., Meheut M., Schmollgruber P., Atinault O., Gauvrit J., Bennehard Q., David C. (2024). From Clean Sky 2 to Clean Aviation: assessment capabilities and down-selection of promising innovative configurations and aero-propulsive integrations, AIAA Scitech January 2024.
- [6] Nguyen Van E., Gauvrit-Ledogar J., Julien C., Paluch B., Ruan L., Moens F., Impact of hydrogen fuel on the overall design of transport aircraft, ICAS conference September 2024.
- [7] Haimes, Robert, et al. "Multi-fidelity geometry-centric multi-disciplinary analysis for design." AIAA Modeling and Simulation Technologies Conference. 2016.
- [8] F. Moens "A Fast Aerodynamic Model for Aircraft Multidisciplinary Design and Optimization Process.", MDPI Aerospace / Special Issue "Aerodynamic Design", Aerospace 2023, 10, 7. https://doi.org/10.3390/aerospace10010007.
- [9] Lowry J and Polhamus E. "A Method for Predicting Lift Increments Due to Flap Deflection at Low Angles of Attack in Incompressible Flow." NACA TN-3911, 1957.
- [10] Raymer D P. "Aircraft Design A Conceptual Approach." AIAA Education Series, 2nd ed., 1992.
- [11] Gur O, Mason W H and Schetz J A. "Full-Configuration Drag Estimation." Journal of Aircraft, 2010, Vol. 47, No 4, p. 1356-1367.
- [12] Niţă M and Scholz D. "Estimating the Oswald Factor from Basic Aircraft Geometrical Parameters." Deutsche Gesellschaft für Luft-und Raumfahrt-Lilienthal-Oberth eV, 2012.
- [13] Hörner S F. "Fluid Dynamic Drag." 1965, Published by the author (Library on Congress Catalog Card Number 64-19666).
- [14] Haftmann B, Debbeler F J and Gielen H. "Takeoff Drag Prediction for Airbus A300-600 and A310 Compared With Flight Test Results." Journal of Aircraft, 1988, Vol. 25, No 12, p. 1088-1096.
- [15] Torenbeek E. "Synthesis of Subsonic Airplane Design." 1986, Springer-Science+Business Media BV.
- [16] Haimes, R., Dannenhoffer, J., Bhagat, N. D., & Allison, "Multi-fidelity geometry-centric multi-disciplinary analysis for design", 2016 AIAA Modeling and Simulation Technologies Conference (lien: https://arc.aiaa.org/doi/epdf/10.2514/6.2016-4007).
- [17] Thomas D. Economon "SU2: An Open-Source Suite for Multiphysics Simulation and Design", AIAA Journal 2016.
- [18] van der Vooren, J., and Destarac, D., "Drag/thrust analysis of jet-propelled transonic transport aircraft; definition of physical drag components," Aerospace Science and Technology, Vol. 8, No. 6, 2004, pp. 545–556. doi:https://doi.org/10.1016/j.ast.2004.03.004.
- [19] Roux, E. "Pour une approche analytique de la dynamique du vol", PhD Thesis, Univ. Toulouse, 2005.
- [20] Priasso V. and Lannoo A., Development of a Mass Evaluation Tool for Classical and Disruptive Aircraft Structures, ICAS conference September 2024.
- [21] S. Tsai and N. Pagano. "Invariant Properties of Composite Materials". Composite Material Workshop March 1968.
- [22] M. Abdalla et al. "Formulation of Composite Laminate Robustness Constraint in Lamination Parameters Space". AIAA Scitech May 2009. 10.2514/6.2009-2478.
- [23] M. Bloomfield et al. "On feasible regions of lamination parameters for lay-up optimization of laminated composites". Proceedings of the Royal Society A: Mathematical, Physical and Engineering Sciences December 2008. 10.1098/rspa.2008.0380.
- [24] Altair OptiStruct, Version 2022.1. Altair Engineering Inc. [Online]. Available: https://2022.help.altair.com/2022.2/hwsolvers/os/topics/solvers/os/user_guide_os_c.htm
- [25] S. de Boer, J. Sodja & R. De Breuker "Continuous Parameterisation of Wing Movable Layout for Design Optimisation" In *20th International Forum on Aeroelasticity and Structural Dynamics, IFASD 2024*, Den Haag, The Netherlands, 2024.
- [26] A. Voß, "Loads Kernel User Guide, Version 1.01," Technical Report DLR-IB-AE-GO-2020-136, Institut für Aeroelastik, Deutsches Zentrum für Luft- und Raumfahrt, Göttingen, Germany, November 2021.
- [27] A. Voß, "An Implementation of the Vortex Lattice and the Doublet Lattice Method," Technical Report

Strut-Braced Dry Wing Concept for Hydrogen-Powered Aircraft

- DLR-IB-AE-GO-2020-137, Institut für Aeroelastik, Deutsches Zentrum für Luft- und Raumfahrt, Göttingen, Germany, Oktober 2020.
- [28] "CS-25 Amendment 27 Review of Aeroplane Performance Requirements for Air Operations and Regular Update of CS-25," EASA, Jan 10 2023. Retrieved 28 March 2023. https://www.easa.europa.eu/en/document-library/certification-specifications/cs-25-amendment-27.